BIOMIMETIC SCAFFOLDS FOR LIGAMENT TISSUE ENGINEERING APPLICATIONS

Fariza Mukasheva, Bachelor in Engineering and Technology

Submitted in fulfillment of the requirements for the degree of Master of Science in Chemical and Materials Engineering

School of Engineering and Digital Sciences
Department of Chemical and Materials Engineering
Nazarbayev University

53 Kabanbay Batyr Avenue,
Nur-Sultan, Kazakhstan, 010000

Supervisor: Cevat Erisken, Ph.D.
Department of Chemical and Materials Engineering

April 2019

Acknowledgments

I wish to thank various people without whom I would not have been able to complete this research. I would like to express my sincere appreciation to my thesis supervisor, Dr. Cevat Erisken, for teaching, providing guidance, comments and recommendations throughout this research work. I have been acquainted with the tissue engineering field and learned many things since I became Dr. Erisken's student. I am particularly grateful to my colleague Amina Amanzhanova for her aid with experiments, unfailing support, and encouragement. Also, I wish to acknowledge the help provided by Laura Khamkhash and Rakhima Shamenova in conducting SEM analysis. Finally, I must express my very profound gratitude to my family and friends for supporting and inspiring me during the compilation of this thesis.

Table of Contents

List of abbreviations

AA	Acetic acid
Ace	Acetone
ACL	Anterior cruciate ligament
CF	Chloroform
DCM	Dichloromethane
DMF	Dimethylformamide
ECM	Extracellular matrix
FA	Formic acid
IPA	Isopropanol
KH_2PO_4	Monopotassium phosphate
LiCl	Lithium chloride
NaCl	Sodium chloride
NaH_2PO_4	Monosodium phosphate
PAA	Poly(amic acid)
PAN	Poly(acrylonitrile)
PEO	Poly(ethylene oxide)
PGA	Poly(glycolic acid)
PC	Poly(bisphenol A carbonate)
PCL	Poly(caprolactone)
PEDOT	Poly(3,4-ethylene dioxythiophene)
PLA	Poly(lactic acid)
PLGA	Poly(lactic-co-glycolic acid)
PLLA	Poly(L-lactic acid)
PSS	Poly(styrene sulfonate)
PVA	Poly(vinyl alcohol)
PVP	Poly(vinylpyrrolidone)
PVDF	Poly(vinylidene fluoride)
SDS	Sodium dodecyl sulfate
SEM	Scanning Electron Microscopy
THF	Tetrahydrofuran
TCD	Tip-to-collector distance

List of Tables

List of Figures

Abstract

Ligament is the soft tissue that connects bone to bone and, in case of severe injury or rupture, it cannot heal itself mainly because of its poor vascularity and dynamic nature. High failure rates of surgical treatment and significant drawbacks of currently available medical approaches brought about a need for alternative treatment approaches such as tissue engineering. It carries the potential to restore the injured tissue functions by utilization of scaffolds mimicking the structure of native ligament tissue.

As the initial structural unit of the ligament, collagen fibrils have a diameter ranging from 20 to 150 nm, which defines the cellular topography, physical, and mechanical properties of the tissue. Currently, ability to fabricate scaffolds with relevant fiber diameter in this range is a significant challenge. The literature review showed a scarcity in terms of bioscaffolds that mimic the foundational unit of tissue consisting of ultra-thin nanofibers with diameter not exceeding 200 nm. To cover the gap, this work aims at: i) investigating the conditions for the fabrication of sub-100 nm fibers, and ii) fabricating aligned scaffolds with bimodal diameter distribution (with two-peaks) resembling the healthy Anterior Cruciate Ligament (ACL) tissue structure, and unaligned scaffolds with unimodal diameter distribution (with a single peak) representing structure of injured ACL tissue. It is hypothesized that such scaffolds can be produced from electrospun polycaprolactone (PCL) solutions in the form of unimodal and bimodal diameter distributions. For testing this hypothesis, various PCL solutions were formulated in acetone and formic acid in combination with pyridine, and electrospun to generate sub-100 nm fibers. Next, this formulation was adjusted for the production of nanofibers with a diameter of greater than 100 nm. Finally, these solutions were combined in the co-electrospinning, i.e., two-spinneret electrospinning, process to fabricate biomimetic scaffolds with bimodal and unimodal diameter distribution.

Findings revealed that electrospinning of 8% and 15% PCL solutions, respectively, resulted in the production of fibers with diameters below and above 100 nm. The combined scaffold exhibited bimodal distribution of aligned fibers with the peaks around 60-80 and 160-180 nm, thus mimicking the collagen fibril diameter distribution seen in healthy ACL tissue.

To the best of my knowledge, this is the first study using the system of acetone and formic acid in combination with pyridine for the production of PCL nanofibers, especially sub-100 nm ultra-thin nanofibers. Another novelty is the fabrication of scaffold with a bimodal

distribution to both qualitatively and quantitatively match the distribution of collagen fibrils seen in healthy ACL tissue.

The biomaterial scaffold fabricated here could be used as a foundation for the development of grafts and has the potential to move the ligament tissue engineering field forward. Moreover, the study outcomes can be applied to the design of not only ligament but also other soft tissue grafts such as tendons and muscles. Therefore, this research is expected to have a society-wide impact because it aims at healing, enhancement of the health condition and life quality of a wide range of patients.

Chapter 1 - Introduction

The thesis topic is related to the tissue engineering area, more specifically, engineering of a synthetically designed scaffold mimicking the collagen fibril diameter distribution of healthy and injured ligament tissues harvested from bovine. Ligament is the viscoelastic tissue that connects bone to bone. The Anterior Cruciate Ligament (ACL) tissue, one of multiple ligament tissues present in the body, at the knee joint functions to stabilize the joint together with other ligaments, tendons and menisci. A damage to ACL tissue in the form of tear or rupture may result in a destabilized joint, eventually leading to osteoarthritis, a significant disease that could potentially end up with the loss of joint. This thesis specifically addresses an unsolved clinical problem due to limited self-healing capacity of ACL, and proposes a formulation for the fabrication of scaffolds representing healthy and injured ACL tissues to be later used as scaffolds for ACL regeneration.

1.1 Ligament tissue

1.1.1 Ligament composition and structure

Ligament tissue consists of cells and extracellular matrix (ECM) which includes collagen, proteoglycans, glycoproteins and elastin [1, 2]. Ligament has limited cell content that includes ligamentocytes and ligamentoblasts that constitute nearly 90-95% of the cellular content, with minor components such as chondrocytes, synovial and vascular cells [2]. Ligament cells play a key role in tissue growth and remodeling [3]. In the cases of stresses and strains, the ligamentocytes can respond to stimuli and adapt the environment [4]. Also, they are known to participate in collagen synthesis. Proteoglycans are presented by decorin, regulating the fibril diameter, and aggrecan, which supplies the tissue with water and resists compression. Glycoprotein tenascin-C helps to transmit mechanical stability, whereas fibronectin is involved in wound healing. Elastin accounts for 2% of the ligament dry weight and takes part in the tissue regeneration after stretching. These components assist the ECM to provide the safe gliding of fibers during mechanical loading, to afford adhesion sites for the cells and bind growth factors [1]. The main component of ligament ACL is collagen making up about 60% of the total ligament dry mass. Collagen is mostly represented by collagen type I, nearly 95% of the total collagen content and about 60-85% of the ECM dry weight, and then types III and V, composing

the remaining 5% [2, 3, 5]. Collagen is the basic unit forming the hierarchical structure of the ligament.

The structure of ligament is based on tropocollagen molecule, produced within a cell and then secreted as procollagen into an ECM [6]. These molecules aggregate to form the main nanostructural unit called fibril with the diameter distribution in the range from 20 to 150 nm [7-9]. From a bunch of fibrils, a collagen fiber of around 1 μm in diameter is formed. A bunch of fibers constitute a primary bundle called sub-fascicle, which in turn forms a secondary bundle called fascicle. Further, according to the hierarchical structure illustrated in figure 1.1.1, a tertiary bundle ends up forming the ligament with the diameter varying from 500 to 1000 μm. The collagen fibers are wrapped around by a thin collagen layer called endoligament which comprises nerves, blood and lymphatic vessels. The hierarchically structured collagen units in the ligament tissue are aligned in the direction of the length of the ligament (figure 1.1.1).

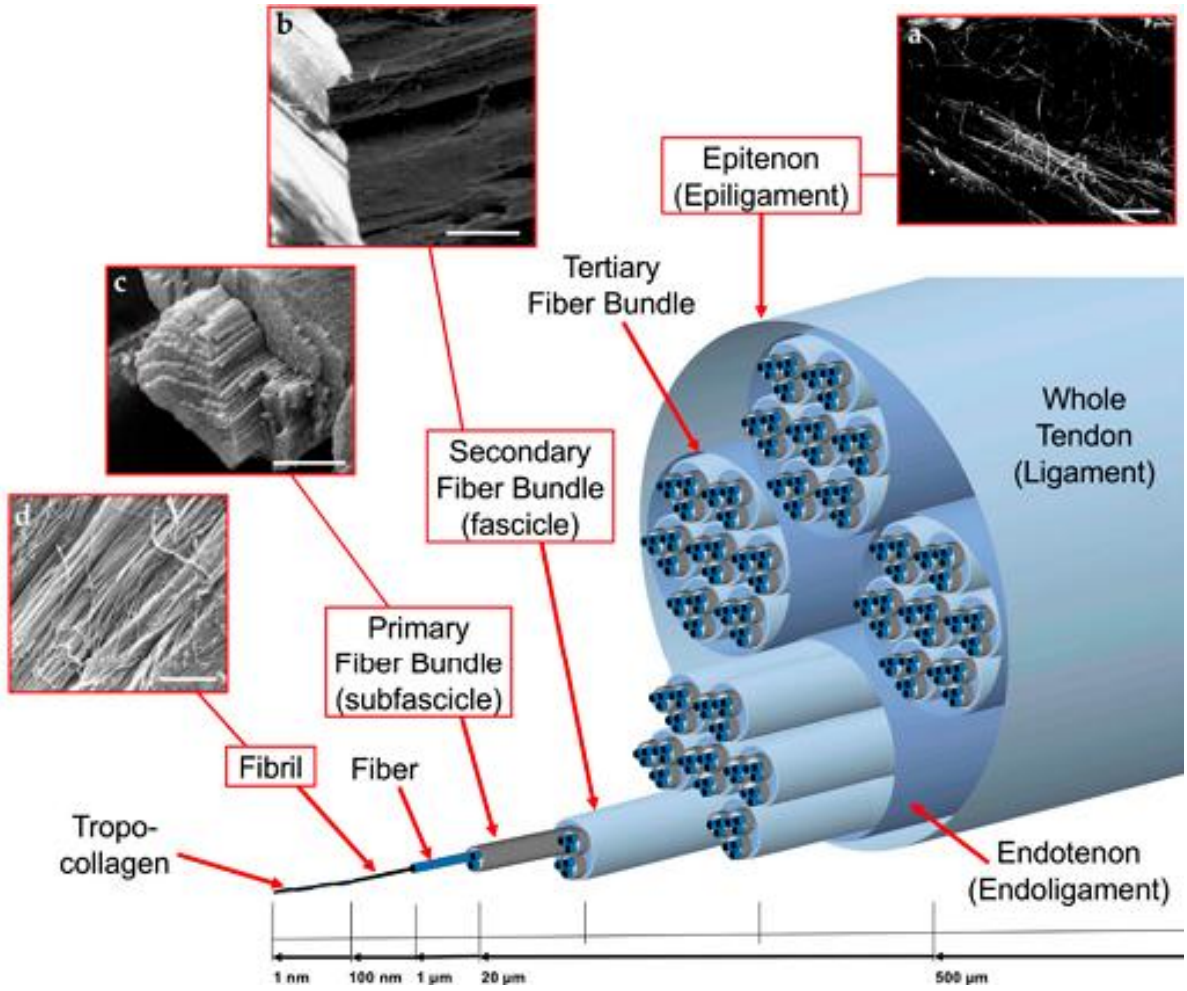

Figure 1. 1. 1: Hierarchical structure of ligament tissue [6]

1.1.2 Ligament function and mechanical strength

Ligaments were naturally designed to withstand large tensile load exerted on the joint to prevent the joint trauma. Such ability is possible owing to mechanical adaptation [4]. The main function of the ligament is to stabilize the joints by preventing and blockage of physically abnormal movement of the joint to minimize the effects of trauma. Also, ligament provides the musculoskeletal system with stability and thereby, contributes to its mobility. Ligament exhibits high mechanical strength and flexibility due to the rope-like structure of hierarchically arranged parallel collagen fibers [2, 8].

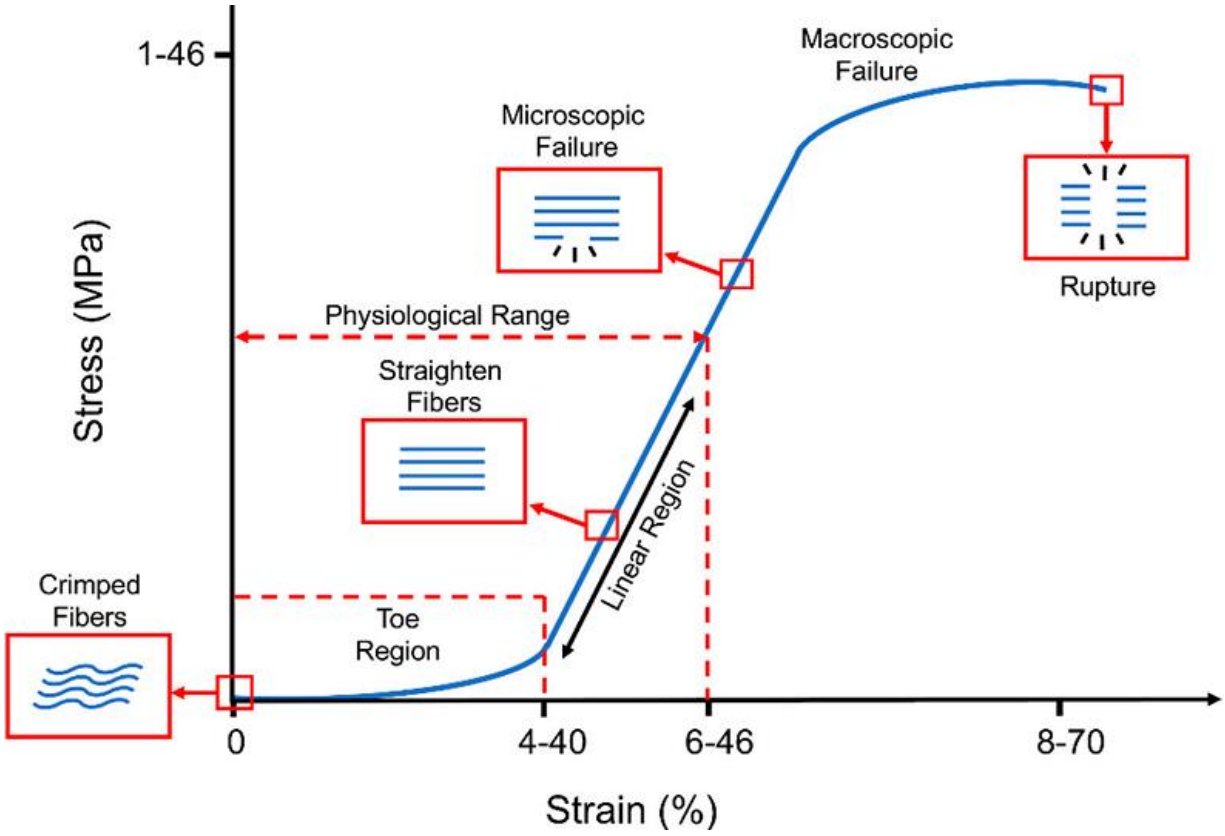

Figure 1. 1. 2: Stress-strain curve of collagen fibers [6]

Initially, the collagen fibers in the tissue are crimped at the resting state, and three deformation regions (toe, linear and rupture) can be distinguished when they are loaded. They are presented in the stress-strain curve that displays the deformation stages of collagen fibers (figure 1.1.2) [5]. In the toe region under low strain, less than 4-40%, fibers start to align and in the linear region they become oriented in parallel to each other. Under a strain up to 6-46%, ligament tissue exhibits elastic behavior, which upon removing the loads returns to the initial

state. Further, additional loading gives rise to the formation of microscopic failure and after that point macroscopic failure, leading to the ultimate rupture, occurs. According to Sensini and Cristofolini [6], the mechanical properties also depend on function and cross-section of specific ligament type. For instance, failure stresses for ligament may vary from 1 to 15 MPa in the flavum and up to 46 MPa in the lateral collateral.

As it is shown in Table 1.1.1, the mechanical characteristics of ligament vary in different ligament types. Ligaments that are responsible for load transmission have high, and ligaments that do not undergo intense force show lower mechanical strengths. Therefore, the mechanical features of a scaffold should suit a certain ligament type [10]. Generally, ligaments can withstand around 40 MPa of strength. The tissue is stronger when the quantity of the fibers organized in the direction of loading is higher. The larger and wider they are, the higher is the tissue resistance to mechanical stress.

Table 1. 1. 1: Mechanical properties of ligament tissues [10]

Ligament type	**Elastic modulus (MPa)**	**Ultimate tensile strength (MPa)**	**Ultimate strain (%)**
Anterior cruciate ligament	65-447	13-46	15-44
Posterior cruciate ligament	150-447	30-36	11-19
Medial collateral ligament	332±58	39±5	17±2
Lateral collateral ligament	345±22	36±3	16±1

1.1.3 Clinical problem, ligament injuries and healing

Ligament injury is one of the most common reason in orthopedic surgery of soft tissues, especially in the elder population and athletes. The structure and function of the healed ligament are not comparable to its healthy form because of the intense synthesis of collagen type III, the disorganized matrix, and the randomly aligned fibers seen upon (scar) healing. Comparing to collagen type I, collagen type III fibers are smaller and thinner, with impaired mechanical strength [4]. So, the weakened ligament brings the patient to a state of limited mobility and an increased risk of repeated rupture.

Conservative treatment includes mobilization and exercises of the damaged body part along with the administration of the non-steroidal drug to mitigate inflammation. If it has failed, surgery becomes the last and most common option. In the surgical method, the necrotic tissue is excised and the ends of the remained tissue are connected by suturing. This leads to the decrement of the ability to withstand mechanical loads [4].

The health problems, related to ligament, affect from 30 to 100 million people worldwide, annually [3, 11]. Ligament is mostly injured as a result of intense physical activity and trauma. The main **clinical problem** consists of inability of ligament to heal itself or respond to drug treatments due to the complex structure, hypocellularity and hypovascularity of the tissue.

The ligament healing process follows three overlapping phases: inflammation, proliferation and remodeling. During inflammation, lasting for about 5 days, the blood clot is formed at the injury site and phagocytic cells migrate there to remove the contaminants and amplify the growth factors. Then fibroblasts help to activate the proliferation phase, which lasts for a few weeks, by the synthesis of ECM components, which forms a strong and granulated tissue. The remodeling phase is the longest one that takes more than a year. Here, the ECM degrades and the granulated tissue becomes more oriented, with collagen fibers organizing themselves parallel to the direction of the applied force. The healing ends with the organization of scar tissue at the wound site. Despite the existence of the native healing mechanism, the formed scar tissue has weaker mechanical and poor viscoelastic properties which result in worsened mobility and high chances of re-rupture.

Different clinical approaches are used to treat ligament injuries. The most widespread is the attachment of ligament to bone with surgical repair, which is based on various suturing patterns providing improved reinforcement [12]. Re-affixed injured tissues are highly susceptible to re-rupture resulting in high failure rates of 20-90% [1, 8, 13].

Another popular repair method is the use of grafts. Especially autografts as in comparison with allografts have lower chances to transmit disease and cause rejection. Unlike surgical attachment, graft patches allow the delivery of biological cues and mechanical support [8]. However, transplantation of grafts also has significant drawbacks such as the limited healing ability or morbidity of the cut site in the ligament tissue from which the implanting graft was harvested. Also a high risk of immunogenic reaction and poor cellularization may exist [5, 16]. Moreover, testing of tensile properties, suture pull-through and shear analysis of the patches made of human, porcine dermis and polyurethane urea proved that the patches have reduced mechanical parameters and cannot fully substitute human tissue [14]. To solve that

problem, the grafts can be replaced by prostheses, but they are unable to mimic the collagenous structure and fail under loading and thus do not show a long-term result [5].

To mimic the native tissue composition, treatment with the growth factors such as BMP-2-7, TGFβ-1-3, FGF using a sponge carrier made of type I collagen was invented [15]. Structural properties increased, but this technique promotes mostly not regenerated ligament, but scar tissue in large amounts. As it was stated earlier, the scar tissue is mechanically weak and increases the chances of re-rupture. Therefore, the inconsistencies in traditional methods necessitate the development of a promising alternative approach such as tissue engineering, possessing the potential to restore complete functions of the injured tissue.

1.2 Tissue Engineering

1.2.1 Ligament tissue engineering

The application of tissue engineering on the ligament is not widespread and is still not used in clinical practice. However, it has good potential to facilitate the understanding and regeneration of injured ligaments [3]. Tissue engineering allows recovering the defective tissue by biochemical stimulation of a patient's repair system with the cells, genes and stimulatory factors that are delivered by a specially designed biomimetic scaffold [4]. The scaffold is produced *in vitro*, then implanted to replace the excised tissue, and degrades simultaneously as the new tissue forms. According to the type of the ECM compound incorporated into the scaffold, there are few types of ligament regeneration, which are, namely, cell-, proteins- and gene-based therapies.

The cell-based therapy can improve the biomechanical and histological features of the tissue to the level comparable to those of healthy tissue. The injection of fibroblasts results in an 86% reduction in pain and improved tissue repair [4]. Mesenchymal stem cells (MSC) derived from bone marrow improve stiffness and reduce the recovery time and re-injury rates.

Genes delivered to the tissue help to change the DNA, induce and regulate the protein production and long-term expression profile. Side effects such as scar tissue formation can also be reduced by genes introduction. However, as nucleic acids are susceptible to degradation and can be destroyed by immunocytes, the use of genes is limited [4, 15].

In the protein based therapy, cytokines and growth factors are in use. The growth factors such as insulin-like, platelet-derived, basic fibroblastic, bone morphogenic proteins (BMP), transforming growth factor-beta (TGF-β) and vascular endothelial growth factor (VEGF) improve cell proliferation and expression of collagen and ECM [4]. Thereby, they increase

cellularity and vascularity. As a result of the facilitated regeneration, the stiffer tissue with significant improvement of the structural and mechanical properties can be achieved. Short half-lives of the growth factors molecules and the inability of the tissue to retain them at the injured site challenge delivery and recovery. To be effective, multiple injections and an elevated level of doses are required.

1.2.2 Biomimetic scaffold

Constructs designed to be utilized in tissue engineering applications are called scaffolds. A scaffold is an engineered replacement of ECM, supporting cell growth and adhesion and providing mechanical strength [16]. Controlled release of cells, genes and proteins is carried out by their insertion in implantable biomimetic scaffolds that not only deliver them to the site of action but also serve as a mechanical support. To reach the effective delivery, the structure and biomechanical properties of the scaffold should mimic the native ligament tissue and provide necessary media for the distribution of proteins. Besides, scaffolds should allow attachment, proliferation, differentiation of cells and deposition of the ECM [17]. To perform these functions, scaffolds should possess non-immunogenicity, suitable mechanical properties and have controlled degradability which depends on the time necessary for tissue recovery. One of the benefits is that there is no need to remove the biodegradable material and thus conduct second surgery [1, 5].

Scaffold properties such as mechanical, structural and biochemical depend on the choice of biomaterial and production techniques. The general requirements for the used materials are the following [6]. They should be biocompatible to encourage cell growth and proliferation and do not cause rejection, toxic and allergic reactions by the donor. Biodegradability is important to allow cells to reconstitute collagen content that will construct new tissue and replace the gradually degrading scaffold [8]. It should be noted that the degradation products must not accumulate in the body and cause inflammation or toxicity. Porosity of biomaterials plays a significant role in cell nutrition, migration and new tissue formation. Considering mechanical properties and structure, the biomaterials have to mimic the native ligament properties presented above.

Biomaterials for ligament regeneration can be divided into natural and synthetic polymers (Table 1.2.1). The natural polymers such as collagen, gelatin, chitosan, hyaluronic acid, alginate and synthetic polymers such as polycaprolactone, polyethylene, PLGA, polyglycolide are commonly used for scaffolds fabrication [2]. Although the biomaterials from

natural polymers [18-22] support faster cell proliferation, they degrade rapidly, are mechanically weak and challenging to treat with latent immunogenicity [3]. Collagen is the main component of ligament, whereas silk possesses high mechanical properties. Their testing [23-25] showed good cellular response but after some time their tensile strength went down.

The synthetic materials have more flexible properties, and accordingly, are often used. They are relatively inexpensive, can be manufactured in large volumes and their degradation rate is controllable. However, they provide lower bioactivity and the products of degradation can be toxic [5]. Among synthetic polymers, polycaprolactone, polyglycolic acid and poly-L-lactic acid are commonly used. The major benefit of synthetic polymers is that they can be obtained by many methods, and the main drawback is the possibility of creating inflammation reaction by the degradation products. In most of application, biocompatible biomaterials are preferred because they exhibit minimal tissue response.

Table 1. 2. 1: Biomaterials for ligament regeneration [16, 17]

Material	**Examples**	**Advantages**	**Disadvantages**
Natural polymers		• High biocompatibility • High bioactivity • Biodegradability • Derived from native ECM	Rapid degradation
	Collagen	Main component of native ligament	Formation of gels
	Silk	High tensile strain and elasticity	Needs for pre-treatment
		Fabrication of micro/nanofibers	
Synthetic polymers	PCL, PGA, PLLA	• Biodegradability • High elasticity • High porosity • Higher mechanical properties • Variety of fabrication methods • Variety of shapes and sizes • Surface functionalization • Fabrication of micro/nanofibers • Large cost-effective scale production	Low bioactivity Long period of degradation Toxic byproducts

In terms of the structure, there are biomaterials made of woven or electrospun fibers [4]. Woven scaffolds have the advantage of the interconnected porous system but cell seeding and proliferation in such systems are complicated [5]. Scaffolds based on electrospun fibers allow good cell adhesion due to the high permeability, surface-to-volume ratio and variable pore size [1]. Also, they allow to reproduce native ECM structure and increase the tensile properties of the material by controlling fiber diameter and organization. Since the scaffold structure should mimic the native tissue and the ligament has fibrous nature, fibrous scaffolds are preferable and used widely. Nanofibers, for instance, have been broadly examined for the repair of different musculoskeletal tissues including ligament, tendon, meniscus, cartilage, intervertebral disk and bone [8].

Mechanical properties such as tensile strength, showing what maximum tension the materials can handle before breaking, and Yong's modulus values, measuring the resistance of the material to elastic reversible deformation in length, also should be considered. From table 1.2.2, it is clear that PGA is mechanically stronger than other presented polymers. Comparatively, PLGA is far weaker but its mechanical properties can be improved by changing the PLA: PGA ratio. Although PCL also exhibits low mechanical features it has an extremely high elongation at rupture up to 1000% [21], which is an important factor for stretchable elastic materials. However along with PLLA, in comparison with other polymers, it has the slowest biodegradation rate lasting up to 2-3 years. PGA degrades in a short period of 2-4 weeks which is not enough for seeded cells to regenerate ligament tissue. Therefore, PGA is often combined with PLA to design the optimal degradation time of PLGA around 2-3 months [26].

Table 1. 2. 2: Biopolymers properties

Polymer	**Molecular weight, g/mol**	**Tensile strength (MPa) [26]**	**Yong's modulus (MPa) [26]**	**Ultimate strain (%) [26]**	**Biodegradation time (months) [27]**
PCL	$(114.14)_n$	20.7-42	210-440	300-1000	24-36
PLLA	$(90)_n$	27.6-50	2700-4140	3.0 – 10.0	>24
PLA	$(90)_n$	21-60	1280	2.5 – 6	12-16
PLGA	$(148)_n$	13.9-16.7	160-240	205-235	2-3
PGA	$(76)_n$	60-99.7	6000-7000	1.5- 20	0.5-1

1.2.3 Fabrication techniques

The developed scaffold should provide a suitable environment for cells to be attached and proliferate, on which the fabrication technique has a significant impact. The widespread scaffold preparation methods are freeze-drying, extrusion, electrochemical alignment, E-jet printing, knitting and electrospinning [3, 7, 12, 21]. Different methods and mechanical properties, shape and structure of the produced scaffolds are presented in table 1.2.3.

The salts, organic solvents and porogens used in the processes confine the infiltration of cells [2]. The migration of cells within the material is highly dependent on the porous structure of the material. Size, shape and interconnectivity of the pores between nanofibers mimic the native tissue morphology [1]. Therefore, the technique producing nanofibers, i.e. electrospinning, is one of the most popular techniques.

Table 1. 2. 3: Scaffolds fabrication techniques [3]

Technique	**Material**	**Shape and structure**	**Mechanical properties**
Freeze drying	Collagen	Sponges, 11-51 mm, 94% porosity, pore size = 62 μm	Elastic modulus = 0.02 MPa, maximum stress = 0.005 MPa
	Collagen/Chondroitin sulfate	Sponge pore size = 53 μm	Linear stiffness = 0.025 N/mm
Electrochemical alignment	Collagen	Collagen tread diameter = 50-100 μm	Ultimate tensile stress = 108 MPa
	Collagen	Woven scaffold, 81% porosity	Stiffness = 23.8 N/mm
E-jet printing	PCL	Fiber diameter = 20 μm	Young's Modulus = 18.9 MPa, ultimate tensile stress = 2.9 MPa, yield stress = 0.8 MPa

Table 1. 2. 3: Scaffolds fabrication techniques (Continued)

Technique	Material	Shape and structure	Mechanical properties
Extrusion	Collagen	Fiber diameter = 137-215 μm	Elastic modulus = 19.3-46.2 MPa
Knitting	PLGA	Scaffold with 3 yarns of 20 filaments with the diameter 25 μm	Failure load = 56.3 N, Stiffness = 0.34-5.80 N/mm
	Silk	Combined knitted silk fibers and sponge, pore size 20-100 μm	Maximum tensile load = 252 N, stiffness = 40 N/mm
	Silk/Collagen	Combined knitted silk fibers and freeze-dried sponge	Failure force = 21.65 N
Electrospinning	Poly(lactic-co-glycolic acid)	Random nanofibers = 568 nm, aligned fibers = 320-1000 nm	EM of random fibers = 107 MPa, aligned = 341-510 MPa
	Poly(L-lactic acid)	Random = 430 nm, aligned = 450 nm	EM of random = 0.63 MPa, aligned = 22.76 MPa
	Poly(L-lactic-co-D,L-lactide)	Crimped fiber diameter = 880 nm, amplitude = 5.2 μm	Crimped fiber modulus = 3 MPa
	Poly (esterurethane urea)	Fibers diameter = 1-2 μm	EM = 4.2-9.2 MPa
	Poly(caprolactone)	Twisted aligned fibers = 200 μm	EM = 30 Mpa, ultimate tensile stress = 17 Mpa
	Poly(L-lactide-co-ε-caprolactone)	Fiber diameter = 643 nm, pore size = 28.5 μm	EM = 2 MPa, ultimate deformation 250%

Freeze-drying offers the possibility of producing the macroporous sponges using the crystals of ice as a porogen [3]. Porosity of the sponges reaches up to 94% which is helpful for cell penetration and transport of nutrients, but inversely affects mechanical properties. Accordingly, scaffolds produced by freeze-drying are not applicable for ligament regeneration due to absence of aligned uniform fibers to mimic collagens. The next method, knitting allows joining the loops of polymer yarns into a multi-hierarchical 3D structure. Pore size of such scaffolds may reach up to 100 μm what is also high and therefore, the knitted threads are often combined with electrospun fibers.

By extrusion, a solution of acidic collagen, the collagen type I fibers with a diameter varying from 100 to 2000 μm were produced. Thanks to the cross-linking process during the extrusion degradation resistance and mechanical properties are enhanced, resulting in an elastic modulus of 19.3-46.2 MPa. Using the electrochemical method and parallel electrodes the aligned collagen type I threads with diameter from 50 to 100 μm and good mechanical properties were obtained. The threads demonstrated mechanical properties similar to those found in native ligament tissue. Namely, ultimate tensile stress about 108 MPa, Young's modulus of 890 MPa and ultimate failure strain of 13%.

E-jet printing of polycaprolactone resulted in the production of fibers with a diameter of 20 μm and relatively poor mechanical properties [12]. Comparing to it, knitting gives the possibility to produce mechanically strong but thick fibers which are not applicable for mimicking the primary structure of native ligament tissue. Mimicking can be achieved by electrospinning that allows getting thin aligned nanofibers, with the diameter ranging from 320 nm and up to 200 μm. The fibers elastic modulus values are also different, but in general, aligned fibers exhibit 3 times higher mechanical properties. Also, it offers the possibility to effectively control the fabrication process.

1.2.4 Effect of fiber diameter

Ligament tissue comprises collagens of different diameters from 10 nm to 1 μm. It is reported that fiber diameter regulates cell differentiation [28]. In the study of the human rotator cuff, fibroblasts seeded on 320±100 nm, 680±180 nm and 1.80±0.16 μm nano-fibrous PLGA (85:15) scaffolds [29], it was demonstrated that after 28 days the cells were more aligned on thicker, rather than thinner fibers. Large fiber diameter favours the cells to elongate and get a spindle shape. In terms of differentiation, aligned fibers favour fibroblasts to spread farther and faster independently of fiber diameter. On the other hand, in comparison with the large-diameter

groups, cell number on the small-diameter fibers was significantly higher [28]. Moreover, in tendon tissue which is structurally similar to ligament, fibroblasts of thinner fibers produced more collagen and proteoglycans, around 0.75 wt% and 0.036 wt% on 320 nm fibers vs. 0.64 wt% and 0.023% on 1.80 μm fibers, respectively, and assisted greater proteoglycan deposition. It was assumed that as the thinner nanofibers simulate the tendon tissue in injured condition, the cells facilitate the synthesis of more matrix components. Whereas larger nanofibers resemble a healthy tendon, so there is no need for the cells to overproduce collagen and proteoglycans. However, when the expression of biomarkers was tested, tenomodulin and collagen I, III, IV reached the highest levels in the microfibrous scaffold probably due to the reduced collagen synthesis. Since tenomodulin is responsible for the uniform and smooth collagen fibrils, the microfibrous scaffold supports the formation of healthy tendon tissue, while the nanofibrous scaffold results in scar tissue. Therefore, likewise in this tendon example, to achieve the ECM synthesis and cell differentiation, for better regeneration of ligament, scaffold with bimodal diameter distribution should be designed and studied.

As collagen fibrils of the injured tissue rearrange poorly, the close mimicking of the native structure is important [7]. Since the ECM composites are presented in the nanometer scale, the materials with nanosize structures should be developed to mimic the tissue. Among the widely used nanostructures, nanofibers are mostly used [17]. These are ultra-thin, interconnected fibers benefit with a high number of pores of variable size so that the cells have the surface area sufficient for their attachment and nutrients can freely exchange.

1.3 Electrospinning

1.3.1 Electrospinning technique

Electrospinning is a method used for the fabrication of ultrathin fibers from different materials, but mainly from polymers, using an electric force. Wang and Ryan [30] consider electrospinning as the only technique that allows generating fibers with diameters from submicrometre to nanometre. The first patent describing the electrospinning process was presented in 1934 by Formhals who invented the apparatus for fabrication of polymer filaments through the induction of electrostatic repulsions. As at that time the method was not commercialized Reneker, Doshi and Chun (1995-1996) revived electrospinning by proving that the technique can produce thin fibers from a variety of organic polymers. Now the method has many modifications and is widely used to generate complex scaffolds applied in tissue engineering.

Electrospun fibers are produced by the effect of high voltage creating an electrically charged polymer jet that dries during extrusion and forms a fiber. An electrospinning setup consists of a pump, a syringe or a tube with spinneret, a voltage supplier, an earthed plate collector or a drum. The pump allows ejecting the polymer solution through the syringe needle/ spinneret at a constant rate. As it is imaged in figure 1.3.1, the voltage supplier is connected to the needle and the collector and transmits a static charge to the polymer solution drop at the needle tip. In the created electric field, the surface tension promotes the migration of the droplet charges toward the collector, so the droplet instead of growing into a sphere becomes distorted.

While charge accumulates, the distortion continues until the droplet reshapes into a conical form called the Taylor cone. When the field strength grows up to the critical value the repulsive electrostatic force overpasses the surface tension and then a fluid jet is ejected from the Taylor cone tip. The following bending of the jet is accompanied by the unstable repulsive electrostatic forces that cause it to loop. In order to mitigate the instability, the discharged jet forms an elongated thin fiber through stretching, thus notably decreasing its diameter, and whipping during which the solvent evaporates and the formed fibers set on the grounded collector/drum.

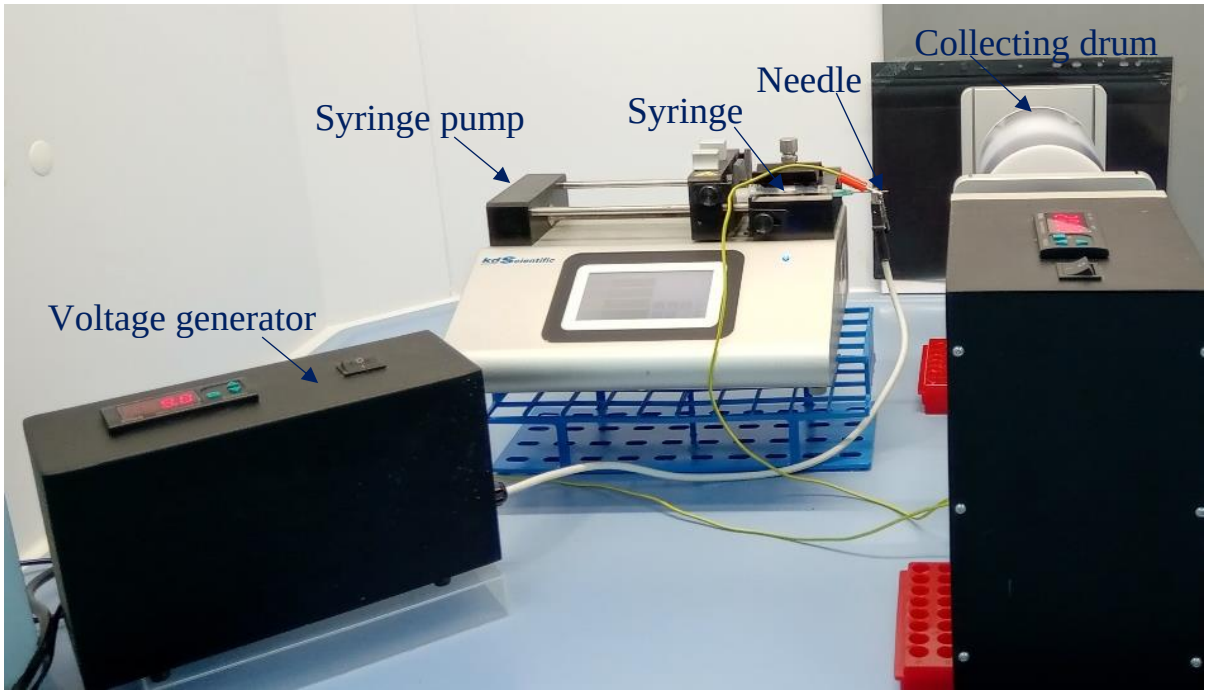

Figure 1. 3. 1: Electrospinning setup

For the fabrication of the electrospun fiber, the majority of soluble high molecular weight polymers can be used. They give the fibers with different morphologies, for example,

ribbons, aligned/unaligned threads, beaded, hollow or core-shell. Also, the fibers can compose 3D porous, randomly oriented mats due to the imbalance in the spinning jet. Moreover, electrospun fibers can be embedded with various additives such as drugs, proteins, growth factors, metals nanoparticles [30].

The solvent volatilization and the elongation of the forming fiber on the product structure. Quick evaporation does not let the highly ordered molecular chains to transform into precise microscale balanced structure. However, solvent-vapour or thermal annealing processes can be used to get a well-defined ordered fibers.

Electrospinning allows changing the arrangement of the fibers. For example, for the production of random fibers, a stationary collector plate is used, and for aligned fibers – a rotating drum. Morphology of fibers can be managed based on the nature of the polymer and solvents and the properties of the polymer solution such as composition, viscosity, concentration, conductivity and surface tension [3]. Moreover, the process parameters influence the material structure. Effect of flow rate, applied voltage, needle size and tip-to-collector distance will be discussed below.

Electrospinning can also be used in combination with other techniques, for example the braiding technique [31, 32]. The aligned nanofiber bundles were electrospun from the polymer solutions. Then three strips of the bundles, stacked on top of others, were braided and knotted manually. In general, the scaffolds showed increased mechanical properties such as yield stress, ultimate stress and Young's modulus (up to 55MPa). Stiffness and flexibility of the scaffold can be controlled by changing the braids quantity. Another variation of electrospinning is the multilayered electrospinning which produces the materials with different layers. For instance, one layer of microfibers can be combined with the following layer of nanofibers, or the layers of various polymers can be alternated. Multilayered PCL scaffolds can enhance cell infiltration in comparison to single-layer scaffolds [13]. Also, other variation called co-electrospinning presents the simultaneous electrospinning of two solutions and allows to fabricate scaffold with the fibers of different diameter [33].

Mostly, electrospinning is used for processing of PCL, PLGA, PLLA or their combination with other synthetic or natural polymers. Fibers of higher diameter exhibit better modulus and reduced resilience. Despite the porous construction of the electrospun material, cells cannot be properly colonized on such fibers due to their high packing density [3].

Cell response can be guided by the appropriate organization of electrospun fibers into random or aligned fibers. The difference between aligned and random fibers was shown on the example of PLGA scaffolds embedded with fibroblasts [34]. The fibers alignment did not affect

cell proliferation within 14 days, but compared to random fibers, mechanical properties of aligned fibers kept longer in culture. The random fibers showed lower elastic modulus (0.107 GPa) comparing to the fibers organized in parallel symmetry (0.34GPa).

The fibers alignment supports the attachment and orientation of cells along the fibers [3]. The cells can recognize the orientation of the fibers and proliferate in the same direction [2]. Testing of the fibroblasts seeded nanofibrous PLGA scaffold on the rat model showed that at day 7, the cells on random fibers appeared round, while the cells on aligned fibers had the more characteristic spindle shape and were aligned along the fibers [35]. Besides, the fibroblasts seeded on aligned fibers generated the highly organized and aligned collagen type I.

1.3.2 Solution parameters

One of the benefits of electrospinning is its controllability that allows regulating fiber structure and diameter. Many important parameters affect the final product and they can be classified as solution dependent, processing and ambient parameters. The parameters depending on the solution are the following: concentration, viscosity, volatility, surface tension, electrical conductivity and dielectric constant. Solution flow rate, applied voltage, needle size and spinning distance refer to the processing parameters. Ambient conditions include temperature and humidity. As the present work aims at fabricating ultra-thin nanofibers, the conditions at which the parameters lead to a decrease of fiber diameter will be discussed further.

The major factor defining fiber diameter is the concentration of polymer solution [36-38]. A solution is naturally prevented from breaking up due to its viscoelasticity as well as surface tension that must be overcome by molecular chain entanglement. The entanglement is sufficient in solutions with a critical minimum concentration denoted as c_e. [39] At higher concentrations, i.e. higher viscosity, the jet struggles to elongate and fiber diameter increases. As the jet does not dry completely, flattened ribbon fibers may form. Also, the solution may not be able to spin and solidify at needle tip thus discontinuing the process. Then the polymer concentration should be decreased, but only to an optimal range. Because at too low concentrations, electrospraying instead of spinning will take place and droplets will be formed, eventually resulting in beaded fibers.

As it is mentioned above, surface tension hinders the jet formation. Increased surface tension is accompanied by higher viscosity and requires the increased electric force which excess leads to unstable jetting and droplets formation. The quality of the fibers can be improved by reducing the surface tension of a polymer solution, for instance, by increasing the

temperature, using the solvent with lower surface tension or addition of surfactants such as Triton-X, SDS [39]. For example, the amphoteric (that carry both cationic and anionic hydrophilic groups) surfactant was used to lower PVA fibers diameter from 250 to 150 nm [37]. However, surfactants may change the final product properties.

The next significant solution parameter is electrical conductivity defined mainly by the properties of a solvent. Electrical charge accumulates easier and enhances the jet elongation in the solution with higher electrical conductivity. Accordingly, for small diameter fibers, more conducting solvents like THF or FA should be used. Also, the salts, such as NaCl, LiCl, NaH_2PO_4, KH_2PO_4, can increase the solution conductivity. Though, too high conductivity results in the jet instability and halting of the process and thus should be avoided [39].

Another solution property for consideration is the volatility of a polymer solution. Solvents with relative volatility should be selected to provide complete evaporation. When the solution is highly volatile, the solvent from the jet surface evaporates too fast. At this time the jet stretching ends and the jet deposits on the collector with the solvent trapped in the fiber core. Further, the trapped solvent diffuses out and leaves the fiber defected with a highly porous or wrinkled surface [37]. Besides, rapidly evaporating solvents do not let the jet to elongate sufficiently during the given time and result in thicker fibers. Hence, the solvents with too low or too high boiling points cannot be used, or be used in combination. Lastly, dielectric constant also needs to be taken into account. Dielectric constant demonstrates the extent to which the solution retains electric charges. The higher the dielectric constant, the higher the stored electrical energy and the thinner fibers can be produced.

1.3.3 Processing parameters

The main process parameter influencing the diameter of fibers is the feed or flow rate of the solution. It specifies the rate at which the pump pushes the syringe with the solution forward and should be adjusted at an optimum value. Too low flow rate makes the Taylor cone depleted and leads to the solidification of the solution in the needle [40]. When flow rate exceeds the optimum range the solution does not have time to be sufficiently charged and form the cone, thus resulting in thicker fibers. By lowering the rate slightly, fibers diameter can be decreased [39]. However, there is a contradiction with the study in which the increased rate did not affect the diameter of PCL fibers [41].

In terms of voltage, the minimum value of voltage necessary for jet formation is governed by the solution viscosity and surface tension. Highly concentrated solutions that

possess high viscosity and surface tension require higher voltage. Although it is reported that an increase in voltage leads to the reduction of fiber diameter the observed effect was minimal [39]. So the effect of voltage on fibers diameter is not clearly defined. Above all, the applied voltage should not be too high, otherwise it will cause the jet instability and droplets formation.

Needles connected to syringes can be used with or without metal spinnerets. The smaller the inner diameter of the needle, the thinner fibers will be produced. Accordingly, the needles of smaller size, with an inner diameter under 1 mm, are more preferable to utilize but only considering the solution viscosity. Highly viscous solutions will block thin needles.

The indicated parameters may be ineffective without fixing the spinning distance. The increase of the distance between the needle and drum increases the flight time. It gives the solvent opportunity to evaporate completely and helps to obtain thinner fibers. For example, when the distance was increased to 14 cm diameter of nylon-6 fibers decreased from 230 to 140 nm [36]. However, the electric field becomes weaker that may lead to thicker and non-uniform fibers. Also, at longer distances the area for collection increases and the yield of fibers lowers. For these reasons, the distance also should not exceed some threshold too much. It refers not only to tip-to-collector distance but to all aforementioned parameters too. The value of the parameter needs to be optimized taking into account the minimum and maximum applicable ranges and interrelation with other factors.

1.3.4 Ambient parameters

The minor factor that affects the solvent evaporation speed and jet stability is the environmental condition. The increase in temperature has a twofold effect. The molecules in solution receive more energy leading to the decrease of surface tension and viscosity and growth of conductivity and thus forming thinner fibers, usually at temperatures beyond 40^0C [39]. However, the evaporation rate at higher temperatures increases with the simultaneous reduction of stretching time and when the difference becomes significant fibers diameter increases.

The increase of humidity promotes the adsorption of water. It decelerates the evaporation rate and provides longer stretching time, thereby decreasing fiber diameter. For instance, finer fibers can be produced if to raise the humidity from 20% to 40% [39]. Further increase beyond 60% results in the fused wet fibers which after drying formed a film. Also, the spinning of a water-insoluble polymer in the highly humid environment results in thicker, defected fibers and is complicated by the needle blockage.

1.3.5 Fabrication of sub-100 nm fibers

Since the ideal values of the mentioned parameters strongly depend on the combination of chosen polymer and solvent, no generally accepted recommendations for the fabrication process exist [42]. To decrease nanofibers diameter, the concentration of the polymer solution should be lowered, but it often results in beads-on-string fibers [43]. As there is a risk of obtaining nanoparticles by decreasing the concentration, the polymer-solvent system should be optimized.

To produce the fibers with a diameter of less than 100 nm, the papers reported about such nanofibers were reviewed. The frequently mentioned solvents and their properties were assembled in Table 1.3.1 [44-46]. According to the table, PCL is highly soluble in AA, CF, DCM and Pyridine, so they are in use for the preparation of solutions in combination with other solvents. As there is a few number of thin nanofibers made of PCL, other polymers such as PLGA, PVA, nylon were also observed and included in Table 1.3.2.

Table 1. 3. 1: Solvents properties [44-46]

Solvent	**Solubility of PCL**	**Dielectric constant at 20^0C**	**Boiling point (^{0}C)**	**Conductivity (S/m)**	**Surface tension, (mN/m)**	**Viscosity (mPa*s)**
Acetone	partial	20.6	56	$5*10^{-7}$	23.3	0.33
Acetic acid	good	6.2	118	$6*10^{-7}$	27.4	1.13
Chloroform	good	4.8	61	$< 1*10^{-8}$	27.16	0.57
DCM	good	9.1	40	$4.3*10^{-9}$	28.12	0.44
DMF	partial	36.7	152	$6*10^{-6}$	35	0.82
Ethanol	bad	22.4	78	$1.4*10^{-7}$	22.3	1.08
Formic acid	partial	58	100.8	$6.4*10^{-3}$	37.67	1.78
Pyridine	good	12.4	115	-	37	0.88
Water	bad	79.7	100	$5.5*10^{-6}$	72.75	0.89

Table 1. 3. 2: Review of fibers with diameters of around 100 nm

Polymer	**Solvent**	**Voltage, (kV)**	**TCD, (cm)**	**Needle, (nm)**	**Rate, (ml/h)**	**Concentration, (%)**	**Fibers diameter, (nm)**
Nylon-4.6 [43]	FA, Pyridine	10	12	-	-	6	25±5
						8	41±10
						10	62±10
						12	110±10
PLA [47]	DMF + LiCl	20	15	-	-	10	20
PAN [48]	DMF	10-25	8-16	-	-	11	38.4
PEO [49]	Distilled water	30	20	-	-	5	89
PLGA [50]	DMF: THF (1: 1)	20	14	18G	0.5	14	50-100
PCL [51]	FA: AA (7: 3)	15-20	10-15	-	-	12.5	73±23
PCL [46]	AA: FA (1: 3)	7.5	15	-	3	10	57±1.5
	(3: 1)						66±1.5
	(1: 1)						83±1.4
	FA						90±1.4
PLGA [52]	THF: DMF (1: 1)	10	5	-	-	15	81.9±16
PVP [53]	IPA: DMF	12-20	12-20	23-21	1-5	5-10	26-96
PCL [54]	CF: DMF (3: 7)	13	10	-	-	4-10	52-80
						13	93-103
PC [55]	DCM:DMF (1:1)	20	15	20G	0.5	14	90

Table 1. 3. 2: Review of fibers with diameters of around 100 nm (Continued)

Polymer	**Solvent**	**Voltage, (kV)**	**TCD, (cm)**	**Needle, (nm)**	**Rate, (ml/h)**	**Concentration, (%)**	**Fibers diameter, (nm)**
PCL [56]	Ace: AA (1: 1)	15	15	21	0.1	20	88
PCL [57]	AA: FA (1: 9)	32	10-20	-	0.5-0.7	14	94±19
Nylon-6 [58]	FA	5	5	-	0.12	15	51±19
PAA [59]	DMAc	30	20	22	-	2	100±21
PVA [60]	PEDOT: PSS	20	15	-	-	20	68
PVDF [61]	Ace: DMF (2: 3)	13	15	15	0.2	12	65

In general, adjusting the polymer concentration allows to control the diameter of fibers. The jets from the solutions of low concentrations elongate and stretch at higher extent. So, most of the concentration of the polymers is between 10 and 15%. Beads were formed on fibers from solutions with a concentration lower than 6% for nylon [43] and 4% for PCL [54]. The minimum concentration at which the fibers were formed is 2% for PAA [59].

As the bead formation is difficult to control, the fibers with bead-on-string were also reported. For example, 5% PEO fibers retained spindle-like beads even after the addition of 0.1-4% PAA (poly acrylic acid) and PAH (poly allylamine hydrochloride) polyelectrolytes which were supposed to dissociate into greatly charged molecules thus enhancing the charge density and stretching of the jet [53]. Also, 5 - 10% PVP fibers morphology improved with the addition of salts, iron (III) and cobalt (III) nitrates, which decreased the beads content from 71% to 7% [53], so the fibers had few beads. Besides, many beads were observed in 50-103 nm PCL fibers from the solutions with less than 10% PCL concentration and few beads were found in 13% PCL solution [54].

To avoid beads production, salts and other substances were added to the solutions. For instance, pyridine [43], silver nitrate nanoparticles of 5-10 nm diameter [50],

tetraethylammonium [52], hexadecyl trimethyl ammonium bromide (HTAB) and SDS [61]. These additives enhance the free electrical charges, assist the ions to carry the current, increase solution conductivity, remove beads and decrease fibers diameter. To note, they were not reported to chemically or structurally change the fibers.

In this research study, PCL was used as the material of construction of scaffolds due to its biocompatibility, biodegradability, high strength and availability. Scaffolds of PCL were fabricated using electrospinning technology because it allows to produce ultra-thin, aligned nanofibers and control the fiber characteristic by optimization of process parameters.

In this study it was hypothesized that the diameter distribution of injured and healthy ACL tissue harvested from bovine can be replicated in a nanofiber structure. To test this hypothesis, this study aims at i) investigating the conditions for the fabrication of sub-100 nm fibers; ii) fabricating aligned scaffolds with bimodal diameter distribution resembling the healthy ligament tissue structure, and unaligned scaffolds with unimodal diameter distribution representing structure of injured ligament tissue.

Chapter 2 – Materials and methods

2.1 Materials

The following chemicals were used in this study: polycaprolactone MW = 80000 g/mol (#440744), acetic acid (#695092), formic acid (#1.10854), acetone (#270725), pyridine (#270970), dichloromethane (#210997), chloroform (#132950), N-N-Dimethylformamide (#319937), triton X-100 (#T9284), sodium dodecyl sulfate (#L3771). All chemicals were supplied by Sigma-Aldrich (Germany).

2.2 Fabrication of ultra-thin nanofibers with diameters below 100 nm

The solvents were used in various combinations and ratios to find the solution leading to beads-free uniform sub-100 nm nanofibers (Table 3.1.1). The solutions were prepared knowing the constants of each solvent and considering the overall dielectric constants to be relatively high. As a result of different solutions screening, an 8% PCL solution was chosen for further scaffold fabrication. A 0.4 v/v % of pyridine was added to a 1 ml solution of acetone and formic acid in the ratio 1:1. Then, 0.08 g of PCL pellets (MW = 80 000 g/mol) was added to the solution and mixed by a magnetic stirrer for 2 hours at 40^0C.

The polymer solution was transferred to the syringe that was stuffed with the 21G needle (inner diameter about 0.514 mm) and settled in the syringe pump (210 Legato, CER201366), with a tip-to-collector distance of 7 cm. Next, the flow rate and voltage values were set at 0.03 ml/hr and 9 kV, respectively. After a few minutes of running, the flow stabilized and the fibers were collected on a piece of aluminum foil that covered the plate and the drum to obtain random and aligned fibers, accordingly. The rotation speed of the drum (with the diameter of 10 cm) was fixed at 2000 rpm.

2.3 Fabrication of nanofibers with diameters greater than 100 nm

Fibers with diameters larger than 100nm were produced from the previously formulated solution except 15% PCL concentration. The volume of pyridine was also increased up to 2%. All other procedures were kept the same as described above.

As only a single voltage generator was used in the existing electrospinning setup, the applied voltage was set to 9 kV and other parameters were manipulated to get the diameter in the desired range. In this regard, the distance from the needle to the collector and needle size were left unchanged. The flow rate was doubled to 0.06 ml/h, and the aligned fibers were collected on the drum at 2000 rpm.

2.4 Bimodal diameter distribution of nanofibers

Once the separate spinning of 8% and 15% solutions were performed, the mat combining the fibers from both solutions was fabricated by co-electrospinning, i.e., two-spinneret electrospinning (figure 2.4.1). Two syringes filled with the solutions were settled in two pumps that were located directly opposite to each other at the same distance of 7 cm from the rotating drum. The needles, both 21G, were connected to the voltage generator with the use of the clips. Then the process was initiated at 9 kV and different values of flow rate, 0.03 ml/h for 8% solution and 0.06 ml/h for 15% solution to simultaneously collect fibers on the drum rotating at 2000 rpm.

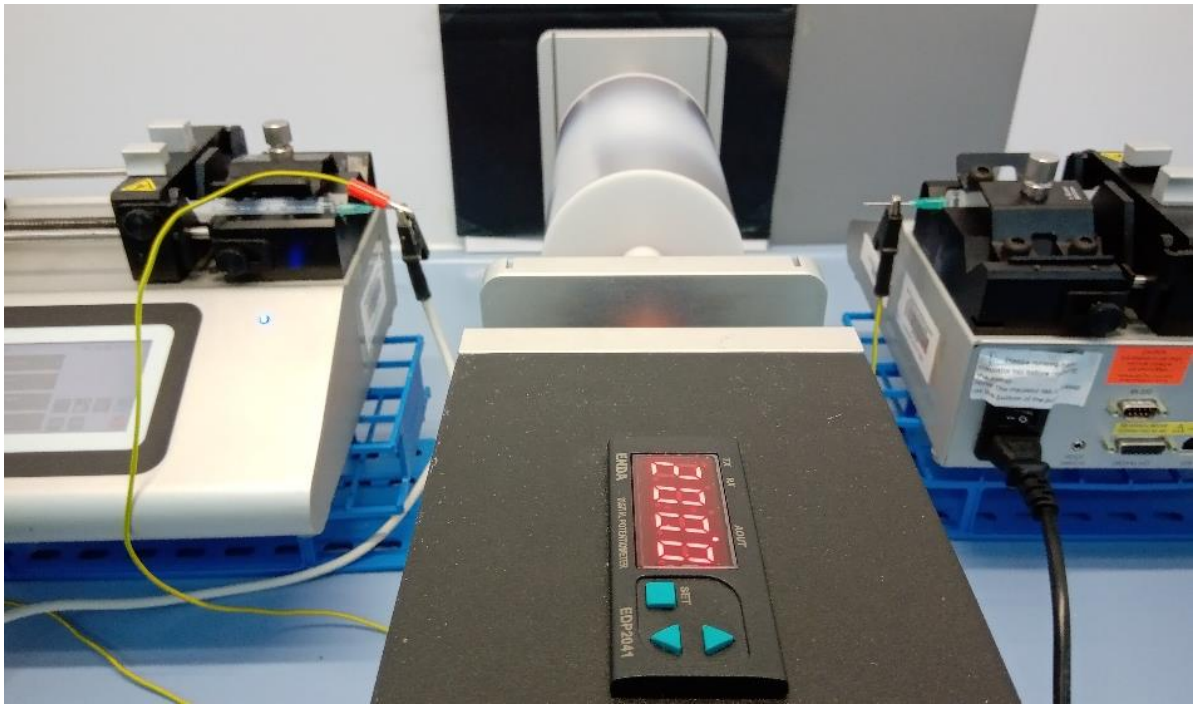

Figure 2. 4. 1: Two-spinneret electrospinning setup

2.5 Scaffold characterization

The samples from 8% random, 8% aligned, 15% aligned, and co-electrospun 8 and 15% solution scaffolds were cut along with the aluminum foil and coated with 10-20 nm layer of gold, depending on the thickness of the sample, at a current equal to 20 mA in the automatic sputter coater (Turbomolecular pumped coater Q150T, Quorum Technologies, UK). Then, the coated samples were analysed on the two different SEMs: Crossbeam 540 (Zeiss, Germany) and JSM-IT200 (JEOL, Tokyo). The micrographs were acquired mostly at an accelerating voltage ranging from 5 to 20 kV, working distance 4-11 mm, probe current around 30 and magnifications values of 300 – 20K.

The average fiber diameter and diameter distribution of 8% random, 8% aligned, 15% aligned and co-electrospun (8&15% solution) scaffolds were calculated using over 200 fibers per image (n=3 images/group, 4 groups). Measurements were performed using 'ImageJ' software (NIH, USA) as described elsewhere [29]. Briefly, each image was segmented with five vertical lines of equal spacing, and fibers intersecting with the verticals were marked. The diameter of these fibers were measured by 'ImageJ', and an average fiber diameter was calculated at a predefined bin range.

For the fiber alignment, the same SEM images of groups were evaluated using 'ImageJ', and results were reported in the range from -90° to +90°.

2.6. Statistical analysis

Comparison of groups of scaffolds with different fiber diameters was performed using student t-test, and significance was achieved at $p<0.05$.

Chapter 3 – Results

3.1 Fabrication of fibers with diameters below 100 nm

Different solutions of PCL in acetone, formic acid and the mixtures of AA: FA, Ace: FA, Ace: DMF, CF: DMF, DCM: DMF were prepared. Concentration of PCL varied from 5 to 30%, flow rate – from 0.005 to 0.1 ml/h, voltage – from 5 to 22 kV and spinning distance – from 5 to 30 cm. Diverse needles of 21, 23, 26 and 30G sizes were utilized. Since various solutions possess distinctive properties discussed in chapter 1.3.2., especially at different processing parameters indicated in chapter 1.3.3, the results vary noticeably. Some solvents formed regular uniform fibers, whereas other solvents favoured electrospraying and formation of droplets. Short descriptions of the produced fibers are presented in table 3.1.1.

Table 3. 1. 1: Solutions used for the fabrication of fibers below 100 nm

Solvent	DC	PCL (% w/v)	Flow rate, (ml/h)	Voltage (kV)	TCD (cm)	Results
AA: FA (1: 1) + 0.4% v/v Pyridine	32.1	7	0.01-0.1	6-20	5	droplets
			0.01	10	5	short fibers, droplets
AA: FA (1: 3)	45.05	10-20	0.01-0.7	5- 15	15.5	droplets
AA: FA (1: 9)	52.82	14	0.01-0.1	7-15	20	non-uniform, few beads
AA:FA (1: 9)	52.82	12	0.01-0.5	5-22	10-20	tiny droplets
AA: FA (1: 9) + 1% v/v Pyridine	-	20	0.2-0.3	8	7	droplets, unstable flow
			0.1	8	7	few beads, 45-130 nm
AA:FA (1: 9) + 1.5% v/v Pyridine	-	30	0.3	20	7	some very thin fibers and droplets, 134-311 nm
Ace + 1% v/v Triton-X	20.6	10	0.1-1	7-20	10-30	discontinued process

Table 3. 1. 1: Solutions used for the fabrication of fibers below 100 nm (Continued)

Solvent	DC	PCL (% w/v)	Flow rate, (ml/h)	Voltage (kV)	TCD (cm)	Results
Ace: FA (1:1)	39.3	10	0.005-0.1	6-20	7	droplets
			0.01	6	5	non-uniform, few beads, 73-270 nm
Ace: FA (1:1)	39.3	8	0.03	6	5	few beads, non-uniform, 40-208 nm
Ace: FA (1:1) + 0.4% v/v Pyridine	-	8	0,03	6	5	uniform, beads-free, 53-87 nm
Ace: FA (1:1)	-	5	0.1	6-10	5-15	spraying, droplets
			0.03	6-7	5	short, thick fibers
			0.01	6	5	lot of droplets, curved non-uniform, 75-180 nm
Ace: DMF (2: 3)	30,26	13	0.05-0.1	7-10	7-10	droplets and beads
			0.01	6.5	7	very beaded, 209-570 nm
			0.01	6.5	15	curved, not uniform, beaded, 300-607
Ace: DMF (2: 3) + 2.48% v/v Triton-X	30.26	20	0.05-0.2	7-8	17	not uniform, beaded, 120-5000 nm
CF: DMF (3:7)+ 0.4% w/v SDS	27.13	13	0.01-0.1	6-12	5-20	droplets
			0.01	8	10	not uniform, beaded, 92-330 nm
CF: DMF (2: 8)	30,32	13	0.005	4.5	12	beaded, 90-110 nm
			0.01	5		
			0.02	7		
CF: DMF (2:8) + 0.4% w/v SDS	30.32	13	0.05	10	12	uniform, beaded ~150 nm
			0.01	8	12	flat, beaded, 160-470 nm
			0.1	10	17	beaded, 140-170 nm

Table 3. 1. 1: Solutions used for the fabrication of fibers below 100 nm (Continued)

Solvent	DC	PCL (% w/v)	Flow rate, (ml/h)	Voltage (kV)	TCD (cm)	Results
DCM:DMF (2:3)	25.66	20	0.1	10	12	280-500 nm
DCM:DMF (4:6) + 0.4% w/v SDS	25.66	15	0.1	9	25	uniform, beads-free, 240-360 nm
			0.1	7	20	very beaded, 400-500
DCM:DMF (4:6) + 0.4% w/v SDS	25,66	12	0.1	7	20	beads free, 100-550 nm
			0.1	9	30	curved, few beads, 151-264 nm
			0.1	10	30	beads, non-uniform, 93-237 nm
			0.05	9	30	few beads, 128-241 nm
			0.1	11	20	few beads, 137-303 nm
DCM:DMF (3:7) + 0.4% w/v SDS	28.42	12	0.03	9	30	beaded, 72-145
		15	0.1	10	25	many beads, 103-270 nm
			0.05	8	20	many beads, 71-210
			0.1	10	30	few beads, 170-294
			0.1	10	35	few beads-on-string fibers, 140-640
FA + 0.4% v/v Pyridine	58	8	0.02-0.1	6-15	5	droplets

From all electrospun solutions, three solvent systems, AA: FA (1:9), CF: DMF (2:8) and DCM: DMF (3:7), resulted in the diameter of the fiber close to 100 nm. Although diameters of these fibers ranged from 45 to 145 nm, they exhibited either small beads (figure 3.1.1 A) or large spindles (figure 3.1.1 B). The only solution allowed to reach the desired ultra-thin nanofibers with a diameter of less than 100 nm was the solution of 8% PCL in the mixture of acetone and formic acid (1: 1) with the addition of 0.4% pyridine.

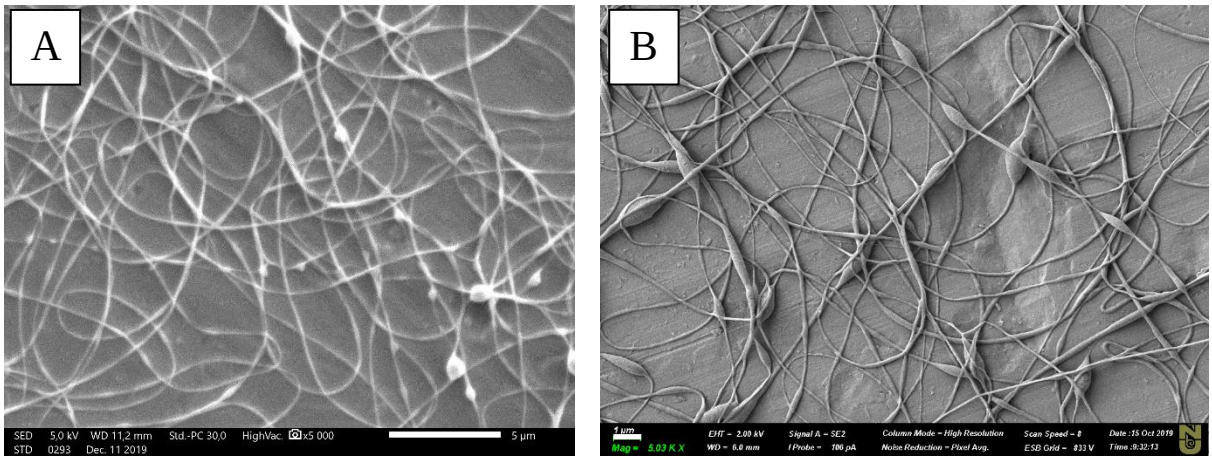

Figure 3. 1. 1: SEM images (x5K) of (A) 12% PCL (DCM: DMF, 3: 7) and (B) 13% PCL (CF: DMF, 2: 8) fibers

To produce the aligned scaffold, 8% solution of PCL was electrospun on a rotating drum. During initial trials, a flow instability leading to an accumulation of a tiny drop at the needle tip was noticed. Then the optimization of the process by the spinning of 8% PCL at different process parameters was attempted (table 3.1.2). A steady state process was reached at the following conditions: 0.03 ml/h flow rate, 9 kV voltage, 7 cm spinning distance and 21G needle. Also, the amount of pyridine was increased from 0.4 to 0.6%. Further, random and aligned fibers from 8% PCL solution were collected and imaged by SEM (figure 3.1.2).

Table 3. 1. 2: Process parameters for 8% PCL (Ace: FA, 1:1)

Pyridine, (% v/v)	**Rate (ml/h)**	**Voltage (kV)**	**TCD, (cm)**	**Needle (G)**	**Results**
0.4	0.1	6	5	21	unstable flow, few beads, 36-130 nm
	0.03	6	10	21	few beads, not uniform, 78-140 nm
	0.03	6	15	21	not uniform, 121-230 nm
	0.1	6-11	15	21	droplets
	0.03	6-9	5	30	unstable flow
	0.03	12	5	30	very tiny droplets
	0.03	8	5	21	large beads, non-uniform, 43-52 nm
	0.03	8	10	21	large spindles, beads, curved, 82-180 nm
0.6	0.03	6	5	21	unstable flow, uniform
	0.03	9	7	21	stable flow, uniform

Table 3. 1. 2: Process parameters for 8% PCL (Ace: FA, 1:1) (Continued)

Pyridine, (% v/v)	Rate (ml/h)	Voltage (kV)	TCD, (cm)	Needle (G)	Results
0.6	0.03	12	7	21	some beads, broken fibers, uniform, about 66 nm
	0.03	17	7	21	many droplets, beads and broken fibers, 67-202 nm

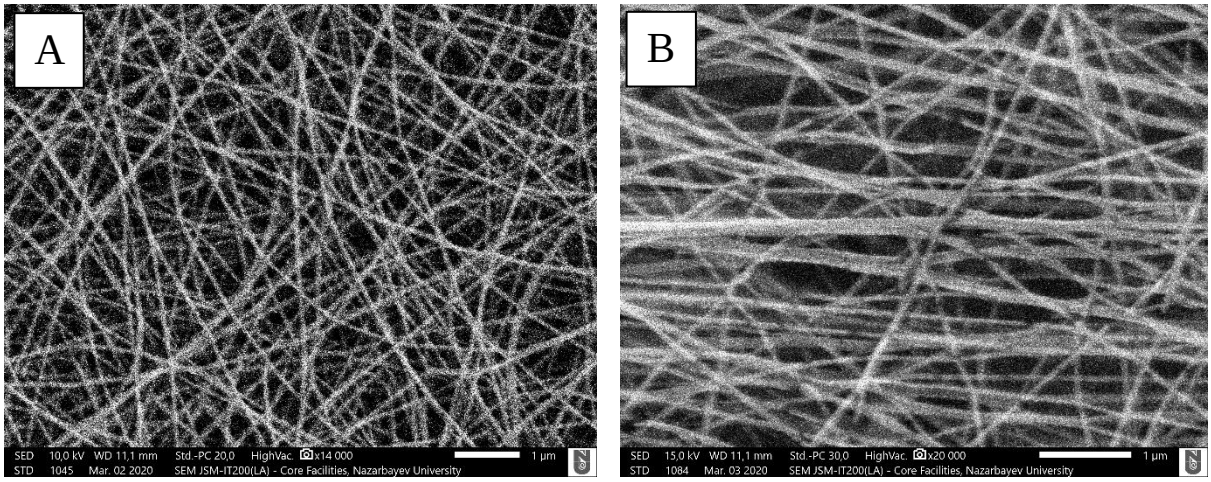

Figure 3. 1. 2: SEM images of 8% PCL fibers (A) random (x14K), (B) aligned (x20K) (Ace: FA, 1: 1)

Three images were used for each group to calculate the average diameter and determine the fibers diameter distribution. The plots for average diameter are shown in figure 3.1.3. Clearly, the random and aligned fibers produced with 8% PCL showed narrow distribution and have almost the same range, from 30 to 100 nm. Also, their average values are similar ($p>0.05$), 55.99±0.62 nm for the random and 60.60±2.26 nm for the aligned fibers.

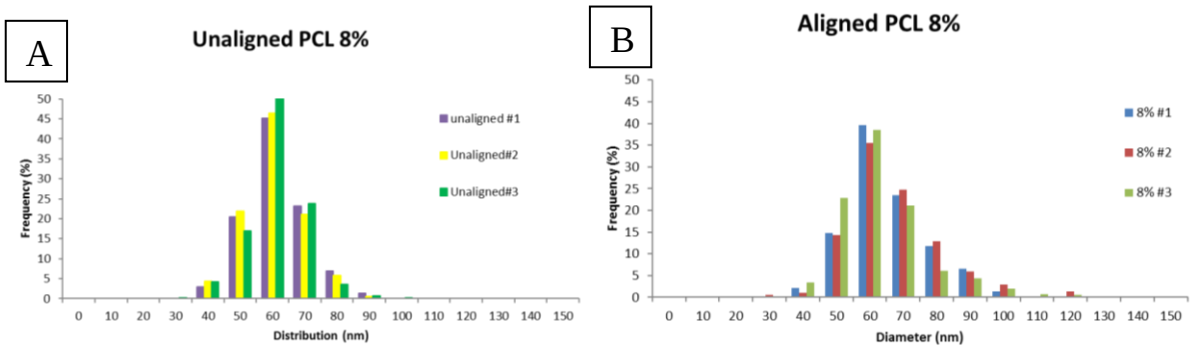

Figure 3. 1. 3: 8% PCL fibers diameter distribution: (A) random, (B) aligned

3.2 Fabrication of fibers greater than 100 nm

The fibers with a diameter greater than 100 nm were generated using higher PCL concentration. A brief characterization of the fibers is given in table 3.2.1.

Table 3. 2. 1: Solutions used for the fabrication of fibers with diameter beyond 100 nm

Pyridine, (% v/v)	PCL (%w/v)	Flow rate (ml/h)	Voltage (kV)	TCD (cm)	Needle (G)	Results
0.6	10	0.03	9	7	21	thin, uniform, 85-120 nm
0.8	12	0.03	9	7	21	some droplets, 95-153 nm
0.8	13	0.03	9	7	21	some curved fibers, uniform, 122-195 nm
2	15	0.06	9	7	21	uniform, 146-244 nm
0.75	15	0.35	20	20	21	large droplets, beads, non-uniform, 88-186 nm
1	16	0.06	9	7	21	curved, some small branches, 120-195 nm
1	17	0.03	18	7	21	not uniform, very curved, 136-1200 nm
1	20	0.03	9	7	21	accumulation at the tip, very curved, 411-1212 nm
		0.06	12-13	7	21	not uniform, 493-2600 nm
1.25	25	0.35	13	15	16	very curved, 1360-1870 nm

As described in the table, an increase in PCL concentration formed fibers with a larger diameter. The solutions beyond 15% resulted in fibers with a diameter comparable to that of 8% solution, however with non-uniform fibers from 16% (figure 3.2.1 A) and very large fibers from 17% (up to 1.2 µm). Further increase of PCL concentration was accompanied by an increase of diameter beyond the expected value. Therefore, a 15% solution was electrospun, and aligned fibers were collected for further characterization (figure 3.2.1 B).

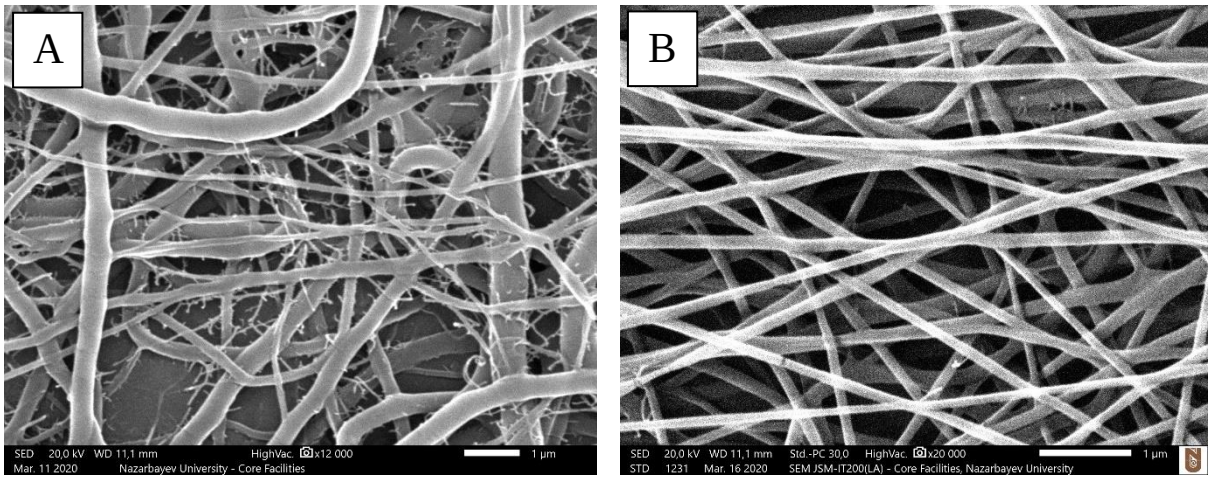

Figure 3. 2. 1: SEM images of (A) 17% (x14K) and (B) 15% (x20K) PCL fibers

Similar to the case of 8% solution, images at magnifications 3K, 10K and 20K were taken and the diameters of each fiber from three images were measured using 'ImageJ'. Then the plot of average diameter distribution was formed (figure 3.2.2). The average diameter of aligned fibers from 15% PCL equals to 149.98±5.19 nm. These fibers possess wide diameter distribution, ranging from 70 to 300 nm. Some fibers with a diameter of about 360 nm were also seen less frequently, which was considered to be insignificant. As a result of the comparison to 8% PCL, the histogram (figure 3.2.3 A) and the line graph (figure 3.2.3 B) show the difference (149.98±5.19 nm versus 60.60±2.26nm, $p<0.05$) in the diameter of the fibers, thus demonstrating the capacity of 8% and 15% PCL solutions to build the scaffold with bimodal diameter distribution, with the peaks at around 60 and 145 nm.

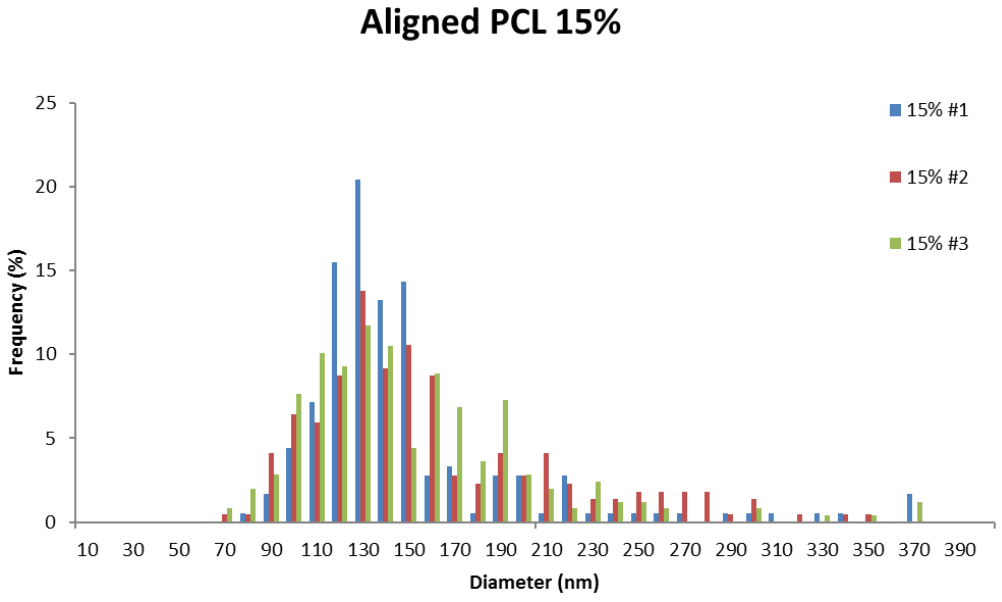

Figure 3. 2. 2: Diameter distribution of 15% PCL (Ace: FA, 1: 1) fibers

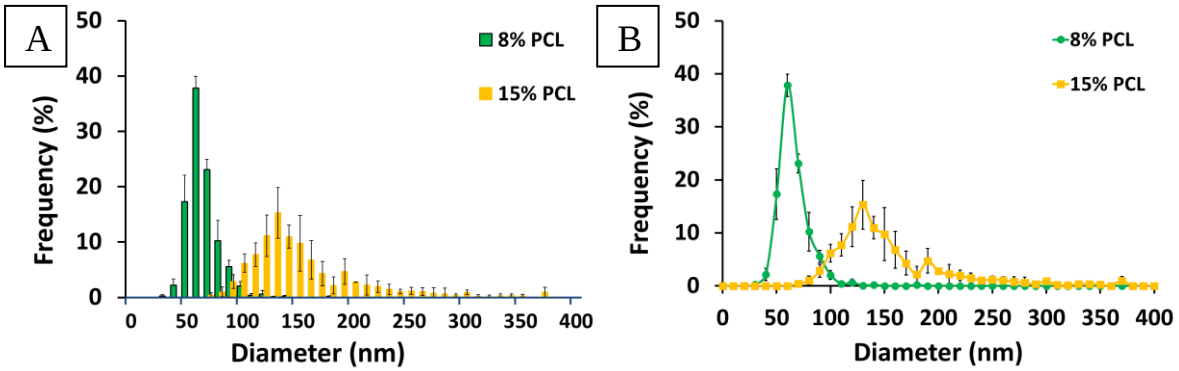

Figure 3. 2. 3: Diameter distribution of 8% and 15% PCL fibers: (A) histogram, (B) line graph

3.3 Fabrication of bimodal scaffold

The 8 and 15% solutions were used for the fabrication of combined fibers by two-spinneret-electrospinning. The morphology of the co-electrospun scaffold is shown in the SEM micrograph (figure 3.3.1 A). As it is depicted in the histogram (figure 3.3.1 B), there are two peaks, at 60-80 nm and 160-180 nm, resulted from both solutions and thus presenting the bimodal diameter distribution of the combined scaffold. Also, the smallest and the largest diameters are seen at about 25 nm and 350 nm, respectively.

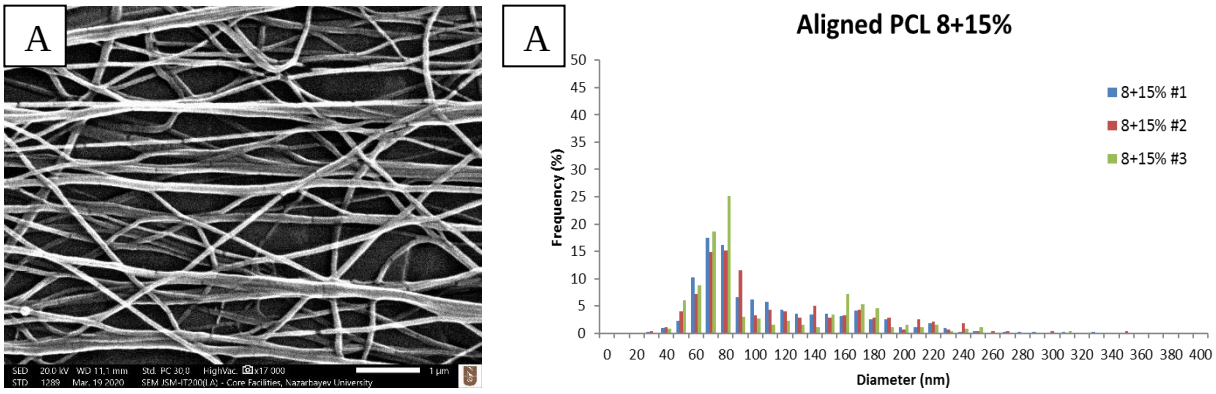

Figure 3. 3. 1: Combined scaffold fibers (A) SEM image (x17K), (B) diameter distribution

The plots of fiber diameters of scaffolds generated from 8% and 15% PCL solutions, and the combined scaffold were displayed in the form of a histogram (figure 3.3.2 A) and the line graph (figure 3.3.2 B). It appears that the diameter range of the co-electrospun scaffold fibers shifted slightly but maintained the general bimodal trend.

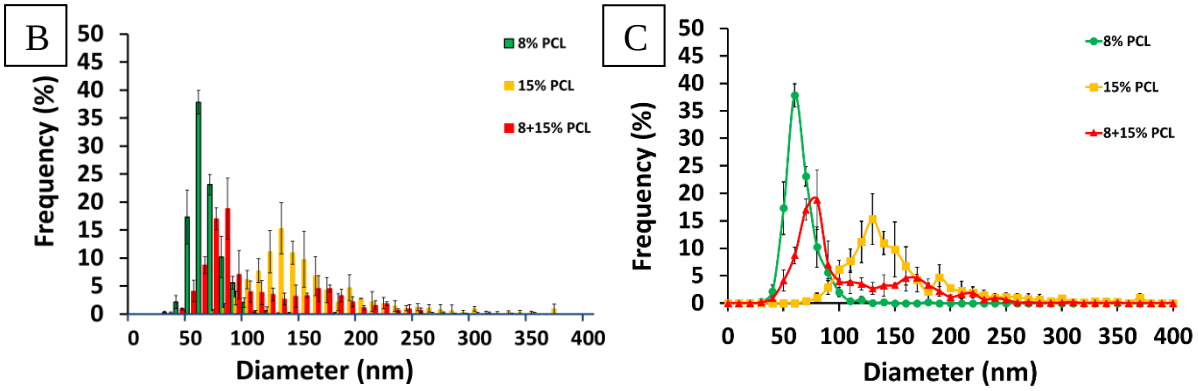

Figure 3. 3. 2: Fiber diameter distribution of combined scaffold (A) histogram, (B) line graph

3.4. Mimicking the fiber diameter distribution of healthy and injured bovine ACL tissue

The fiber diameter distribution of the combined scaffold was compared with the distribution of collagen fibrils of bovine ACL previously studied by Beisbayeva [62]. It can be seen from figure 3.3.3 (A) that the designed bimodal scaffold matches with the collagen fibril distribution of healthy ACL. The average diameters were calculated as 105.42±3.74 nm and 137.43±15.90 nm for bimodal scaffold and healthy ACL tissue, respectively, $p>0.05$). Also, the distribution of random fibers generated with 8% solution was qualitatively similar to the injured ACL tissue (figure 3.3.3 B). Also, the average diameter of the fibers formed with 8% solution and that of collagens in injured ACL were found to be 55.99±0.62 nm and 92.67±10.79 nm, respectively, $p<0.05$).

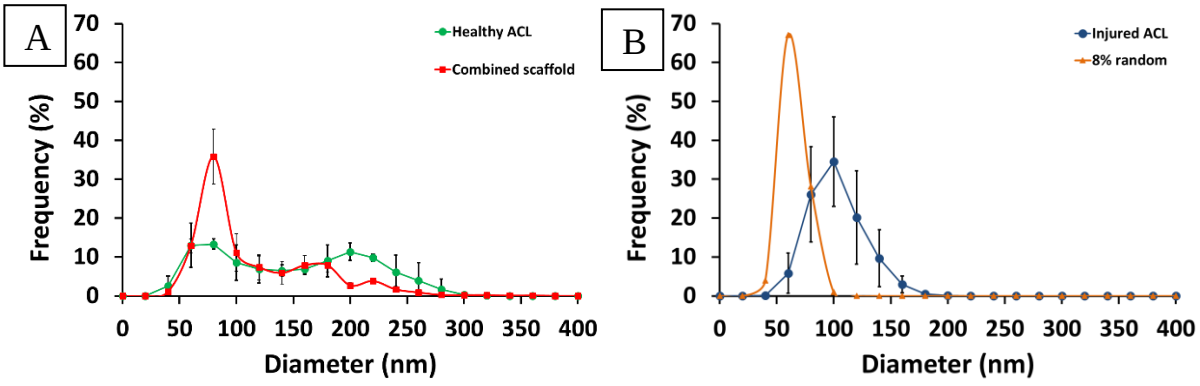

Figure 3. 3. 3: Diameter distribution of (A) combined scaffold fibers and healthy ACL collagen fibrils, (B) 8% PCL random fibers and injured ACL collagen fibrils

Chapter 4 - Discussion

The study investigated the solvents, solutions and process parameters that allow the fabrication of sub-100 nm PCL nanofibers. Production of nanofibers with a diameter of less than hundreds of nanometer remains as a challenge [47] because quality of fibers is often compromised by the formation of beads in the form of droplets or spindles on fibers. They are formed when a solvent does not have sufficient time to evaporate so that the jet does not completely dry before reaching the collector. It is also highly dependent on polymer concentration. Here, two possibilities need to be considered. When the concentration and, as a result, the viscosity is low, the fiber cannot keep its shape and results in electrospraying. That is what happened with 8% PCL in FA as it was too diluted. On the other hand, when the polymer concentration increases, the surface tension of the solution increases too. This causes instability that forces a solution to take a smaller surface area per unit mass thus converting the jet into droplets [47]. So, the equivalent concentration of a solution needs to be determined.

As it is indicated in table 3.1.1, 5% of PCL was sufficient for the production of fibers from Ace: FA (1:1) solution, but the fibers were beaded. The increase of the concentration up to 8% was accompanied by the decrease of beads quantity, however, did not produce bead-free uniform fibers. The aimed fibers were obtained when pyridine was added to the solution, which, comparing to the solution without pyridine, resulted in beads-free fibers with the narrow diameter range from 40 to 100 nm and average diameter about 56.99±0.62 nm for the random and 60.60±2.26 nm for the aligned fibers ($p>0.05$). Slight yet insignificant difference between the random and aligned fibers can be explained by the substitution of a plate by the drum. The high rotational movement of the drum causes the solvent to evaporate faster and the jet to dry earlier than in the case of collecting on the plate, thereby it giving rise to thicker fibers.

Pyridine is a weak base, which in the reaction with weak formic acid generates an organic salt, thus enhancing the accumulation of the ions carrying the current and the electrical conductivity growth. The effect of pyridine was demonstrated when it was added to the solution of nylon-4.6 in formic acid [43]. An addition of 0.3% by weight pyridine increased the conductivity of an 8% solution by almost 26% and prevented the formation of beads. No impact of pyridine on surface tension and viscosity was observed.

In terms of the properties of the used solvents, PCL is only partially soluble in both acetone and formic acid, hence the solution was heated up to 40^0C to increase solubility. The

solvents that partially or fully dissolve PCL such as chloroform, DCM, THF were found to produce either microfibers or beaded nanofibers [46]. It was previously shown that the relatively low values of dielectric constant from 4.8 to 9.1 account for the large diameter [46]. The solutions with lower dielectric constants do not strongly uphold the electrostatic field and cause microfibers. The increase of the solution's dielectric constant, by addition of the solvents with higher dielectric constants, contributes to the elevated electrical energy and the thinner fibers generation.

The dielectric constants of the certain solutions were calculated and it was observed that the solutions with the constants equal to 28 or above produced thinner fibers with few beads (table 3.1.1). The dielectric constant of Ace: FA (1:1) solution, which is about 39.3, is in the effective range equal to 19 or higher [46]. However, it does not show a strict correlation with the results of spinning as the fibers were formed from solutions with both lower and higher dielectric constants (Table 3.1.1).

The experiment with spinning of 10% PCL solution in acetone alone demonstrated that low boiling point (b.p. ~ 56°C), that is to say high volatility of the solvent, hinders fiber formation. Acetone evaporated too fast, thus depriving the extruded jet an opportunity to stretch and reach the collector. This causes the jet to dry at the needle tip and discontinue the spinning process. In contrast, formic acid has high b.p. ~ 100.8°C and low volatility, which is also not desirable as such solvents may not have time to evaporate, remain in the fibers and then produce thick and flat fibers. But mixing of acetone and formic acid resulted in the averaged acceptable volatility.

Although the surface tension and viscosity of acetone and formic acid also vary significantly and were optimized by mixing, they are still governed by polymer concentration which is defined by molecular weight. Here, a discrepancy in the appropriate molecular weight was found out. According to Chaurey [56], 15% PCL (MW = 80000 g/mol) solution in Ace: AA (1:1) formed non-uniform fibers with mean diameter about 388 nm and a wide diameter range from 200 to 1400 nm. Unlike, electrospinning of the same solution of PCL but with MW = 45000 g/mol allowed to obtain ~ 88 nm fibers (Table 1.3.2). For this reason, PCL with higher MW was recommended for the production of microfibers, whereas lower MW PCL - for nanofibers. However, current study shows that 80000 g/mol PCL is suitable for the fabrication of ultra-thin nanofibers.

Considering the process parameters, flow rate seems to be the most important factor. Although the chosen rate of 0.03 ml/h is very low, it offered more uniform fibers without droplets which were formed at 0.1 ml/h. As was stated in the previous chapters, a higher flow

rate favours the generation of thicker fibers. Fibers also could enlarge because of the elongation of the tip-to-collector distance. However, a small increase of the tip-to-collector distance did not substantially affect the diameter of the fibers from 8% PCL which were, at first, collected at 5 cm distance. Then to improve the alignment, the distance was increased up to 7 cm which was followed by the necessity to increase the applied voltage from 6 kV to 9 kV. The reason is that the electric field was extended and now required a higher voltage to form a jet and maintain its spinning for longer periods.

To produce fibers with a diameter of nearly 200 nm, the concentration of PCL in Ace: FA (1: 1) was increased. As expected, more concentrated solutions formed larger fibers. For instance, the fibers with nearly 125 nm were generated from 13% solution and 150 nm – from 15% solution, but the stable growth of diameter finished at 16% solution which formed the fibers similar to 15% solution fibers. Then probably due to the exceed of the optimal range of the earlier discussed critical minimum concentration, the sharp boost of diameter was observed in fibers from 17% solution, up to 1200 nm. Further increase of concentration led to the formation of thicker fibers, diameter of which reached roughly 1500 nm (table 3.2.1), and hence were not in the desired range. The same case was also noted by Bolgen [54] when an increase of PCL concentration from 13 to 15% resulted in a sharp increase of the diameter of the fibers from 100 nm to 250 nm, respectively. Therefore, a 15% solution was selected and the fibers with an average diameter range 149.98±5.19 nm were fabricated.

Higher concentration, i.e. higher viscosity, allows to increase the flow rate and speed the process up. The flow rate of 15% solution was increased up to 0.06 ml/h. Further increase, at 0.35 ml/h, resulted in higher voltage, 20 kV, and larger distance, 20 cm, which altogether formed thin but non-uniform fibers with droplets and beads. Since the co-electrospinning setup had only one voltage supplier, voltage value 9 kV used for an 8% solution remained unchanged. Tip-to-collector distance was also the same as for an 8% solution because its modification may cause differences in the alignment of the fibers.

When 8% and 15% solutions were found suitable they were co-electrospun simultaneously at the previously defined parameters and the fibers were collected onto the rotating drum. As it is depicted in figure 3.3.1, the fibers look partially aligned. The diameter ranges from 40 to 250 nm and the frequency of thinner fibers ~ 60-80 nm is three times higher than thicker fibers ~160-180 nm. However, the latter fibers were electrospun at a rate two times higher and were expected to have a high frequency. The possible reason may be the failure of the clip connecting two needles (figure 2.4.1) to appropriately transmit the given voltage.

In comparison with the separately electrospun 8% and 15% fibers the diameter of combined fibers is slightly increased from 60 up to 80 nm and from 145 up to 180 nm (figure 3.3.2). However, this increase turned out to be beneficial when the diameter distribution of these fibers and the collagen fibrils from healthy and injured ACL [62] were put together. According to figure 3.3.3 the diameter of the fibers distribution coincides with the fibrils of healthy tissue at 80 and 180 nm peaks. In addition, the thinner part of the scaffold, i.e. 8% solution fibers, also mimics the injured tissue, thus making it possible to be used as a graft able to substitute the injured tissue until the healthy tissue will be fully regenerated.

Another challenge was the characterization of the morphology of the fiber by SEM because the samples under the electron beam become melted and destroyed which affects their evaluation. PCL has charge density nearly 0.002 C/cm^2 and is extremely sensitive to the electron beam [63] which disrupts the nanofiber. It is stated [43] that electron radiation can break the nanofibers structure as the polymer molecules are not stable. Especially ultra-thin fibers are highly delicate and cannot bear the radiation for the period required to focus at higher magnification.

Overall, the ultra-thin nanofibers with diameters below 100 nm were obtained and a scaffold with bimodal diameter distribution mimicking healthy ligament tissue was fabricated. The appropriate solvents and process parameters for the design of sub-100 nm fibers were investigated and validated. The beads-free fibers with an average diameter range of 60.60±2.26 nm were produced. Then the solution was used in combination with the same solution of higher concentration in the co-electrospinning process. The scaffold with bimodal diameter distribution replicates the collagen fibril diameter distribution of healthy ACL tissue, with two peaks, about 80 and 180 nm. Similarly, the randomly oriented fibers with an average fiber diameter of 55.99±0.62 nm mimics the injured ACL tissue.

Chapter 5 - Conclusion

The bimodal scaffold generated in this study is expected to serve as a graft for ligament regeneration because it closely mimics structural properties of healthy ACL tissues. Also, the scaffold representing injured ACL can be used as cell substrates to understand the behaviour of cells following injury. Therefore, as a further study, it is recommended that both scaffolds should be tested by seeding ligament cells and evaluating their behaviour on these scaffolds. Findings of this study and forthcoming studies using these scaffolds will undoubtedly have significant impact on the efforts of orthopaedic research community to solve an important societal and economic healthcare problem related to ligament injuries.

References

[1] Anjana, J., *et al.*, "Nanoengineered Biomaterials for Tendon/Ligament Regeneration," Chapter 4 in Mozafari, M., *et al.*, eds., "Nanoengineered biomaterials for Regenerative Medicine," 1st ed., Elsevier Inc., Amsterdam, Netherlands, pp. 73-93 (2019).

[2] Cross, L. M., *et al.*, "Nanoengineered Biomaterials for Repair and Regeneration of Orthopedic Tissue Interfaces," Acta Biomaterialia, 42, pp. 2-17 (2016).

[3] Beldjilali-Labro, M., *et al.*, "Biomaterials in Tendon and Skeletal Muscle Tissue Engineering: Current Trends and Challenges," Materials, 11 (7): 1116 (2018).

[4] Khan, W., "Ligament Tissue Engineering" in Oliveira, J., and R. Reis, "Regenerative Strategies for the Treatment of Knee Joint Disabilities. Studies in Mechanobiology," Tissue Engineering and Biomaterials, 21, Springer, Cham (2017).

[5] Alshomer, F., *et al.*, "Advances in Tendon and Ligament Tissue Engineering: Materials Perspective," Journal of Materials, 968151 (2018).

[6] Sensini, A., and L. Cristofolini, "Biofabrication of Electrospun Scaffolds for the Regeneration of Tendons and Ligaments," Materials, 11: 1963 (2018).

[7] Wu, Y., *et al.*, "Fiber-based Scaffolding Techniques for Tendon Tissue Engineering," Journal of Tissue Engineering and Regenerative Medicine, 12, pp. 1798-1821. (2017).

[8] Zhang, X., *et al.*, "Biomimetic Scaffold Design for Functional and Integrative Tendon Repair," J Shoulder Elbow Surg., 21(2), pp. 266-277 (2012).

[9] Woo, S. L-Y., *et al.*, "Functional Tissue Engineering of Ligament and Tendon Injuries," Chapter 67 in Atala A., *et al*., eds., "Principles of Regenerative Medicine," 3rd ed., Academic Press, Cambridge, US, pp. 1179-1198 (2018).

[10] Santos, M. L., *et al*., "Biomaterials as Tendon and Ligament Substitutes: Current Developments" Regenerative Strategies for the Treatment of Knee Joint Disabilities, 21, pp. 349-371 (2016).

[11] Gaspar, D., *et al.*, "Progress in Cell-based Therapies for Tendon Repair," Advanced Drug Delivery Reviews, 84, pp. 240-256 (2014).

[12] Wu, Y., *et al.*, "Direct E-jet Printing of Three-dimensional Fibrous Scaffold for Tendon Tissue Engineering," J Biomed Mater Res B: Appl Biomater, 105(3), pp. 616-627 (2017).

[13] Chainani, A., *et al*., "Multilayered Electrospun Scaffolds for Tendon Tissue Engineering," Tissue Engineering. Part A 19 (2013).

[14] Chaudhury, S., *et al.,* "Tensile and Shear Mechanical Properties of Rotator Cuff Repair Patches," J Shoulder Elbow Surg., 21(9), pp. 1168–1176 (2012).

[15] Shearn, J. T., *et al.,* "Tendon Tissue Engineering: Progress, Challenges, and Translation to the Clinic," J Muskuloskeletal Neuronal Interact, 11(2), pp. 163-173 (2013).

[16] Font Tellado, *et al.,* "Strategies to Engineer Tendon/Ligament-to-Bone Interface: Biomaterials, Cells and Growth Factors," Adv Drug Deliv Rev., 94, pp. 126-140 (2015).

[17] Deng, M., *et al.,* "Nanostructured Polymeric Scaffolds for Orthopaedic Regenerative Engineering," IEEE Transaction on Nanobioscience, 11(1), pp. 3–14 (2012).

[18] Caliari, S. R., and B. A. Harley, "The Effect of Anisotropic Collagen-GAG Scaffolds and Growth Factor Supplementation on Tendon Cell Recruitment, Alignment, and Metabolic activity," Biomaterials, 32(23), pp. 5330–5340 (2011).

[19] Grier, W. K., *et al.,* "The Influence of Pore Size and Stiffness on Tenocyte Bioactivity and Transcriptomic Stability in Collagen-GAG scaffolds," Journal of the Mechanical Behavior of Biomedical Materials, 65, pp. 295–305 (2017).

[20] Müller, S. A., *et al.,* "Effect of a Simple Collagen Type I Sponge for Achilles Tendon Repair in a Rat Model," The American Journal of Sports Medicine, 44(8), pp. 1998–2004 (2016).

[21] Li, G., *et al.,* "Silk-based Biomaterials in Biomedical Textiles and Fiber-based Implants," Advanced Healthcare Materials, 4(8), pp. 1134–1151 (2015).

[22] Ghiasi, M., *et al.,* "Silk Fibroin Nano-Coated Textured Silk Yarn by Electrospinning Method for Tendon and Ligament Scaffold Application," Nano Hybrids, 7, pp. 35-51 (2014).

[23] Juncosa-Melvin, N., *et al.,* "The Effect of Autologous Mesenchymal Stem Cells on the Biomechanics and Histology of Gel-Collagen Sponge Constructs Used for Rabbit Patellar Tendon Repair," Tissue Engineering, 12, pp. 369–379 (2006).

[24] Kew, S., *et al.,* "Regeneration and Repair of Tendon and Ligament Tissue Using Collagen Fibre Biomaterials." Acta Biomaterialia, 7, pp. 3237–3247 (2011).

[25] Hennecke, K., *et al.,* "Bundles of Spider Silk, Braided into Sutures, Resist Basic Cyclic Tests: Potential Use for Flexor Tendon Repair," PLOS ONE, 8(4), e61100 (2013).

[26] Farah, S., *et al.,* "Physical and Mechanical Properties of PLA, and their Functions in Widespread Applications - A Comprehensive Review," Advanced Drug Delivery Reviews, 107, pp. 367-392 (2016).

[27] Gorth, D., *et al*., "Matrices for Tissue Engineering and Regenerative Medicine," chapter 10 in Lysaght, M., and T. J. Webster, eds., "Biomaterials for Artificial organs," Wooddhead Publishing Series in Biomaterials, pp. 270-286 (2011).

[28] Jenkins, T. L. and Little, D. "Synthetic Scaffolds for Musculoskeletal Tissue Engineering: Cellular Responses to Fiber Parameters," Regenerative Medicine, 4:15 (2019).

[29] Erisken, C., *et al.,* "Scaffold Fiber Diameter Regulates Human Tendon," Tissue Engineering: Part A, 19(3-4), pp. 519-528. (2013).

[30] Wang, L., and J. Ryan, "Introduction to Electrospinning" Chapter 1 in Bosworth, L.A., and S. Downes, eds., "Electrospinning for Tissue Engineering", Woodhead Publishing Limited, Cambridge, UK, pp. 3-33 (2011).

[31] Barber, J., *et al.,* "Braided Nanofibrous Scaffold for Tendon and Ligament Tissue Engineering," Tissue Engineering. Part A, 19 (11-12) (2011).

[32] Jayasree, A., *et al.,* "Bioengineered Braided Micro–Nano (Multiscale) Fibrous Scaffolds for Tendon Reconstruction," Biomaterials Science & Engineering, 5(3), pp. 1476–1486 (2019).

[33] Ladd, M.R., *et al.,* "Co-electrospun Dual Scaffolding with Potential for Muscle-Tendon Junction Tissue Engineering," Biomaterials, 32, pp. 1549-1559 (2011).

[34] Moffat, K. L., *et al.,* "Novel Nanofiber-based Scaffold for Rotator Cuff Repair and Augmentation," Tissue engineering. Part A, 15(1), pp. 115–126 (2009).

[35] Xie J, *et al.,* "Aligned-to-random" Nanofiber Scaffolds for Mimicking the Structure of the Tendon-to-bone Insertion Site," Nanoscale, 2(6), pp. 923–926 (2010).

[36] Khoo, W., and C. T. Koh, "A Review of Electrospinning Process and Microstructure Morphology Control," ARPN Journal of Engineering and Applied Sciences, 11(12), pp. 7774–7781 (2016).

[37] Valizadeh, A., & S. M. Farkhani, "Electrospinning and Electrospun Nanofibers," IET Nanobiotechnology, 8 (2), pp. 83–92 (2014).

[38] Xue, J., *et al.,* "Electrospinning and Electrospun Nanofibers: Methods, Materials, and Applications," Chemical Reviews, 119, pp. 5298–5415 (2019).

[39] Williams, G. R., *et al*., "Nanofibers in Drug Delivery," UCL Press (2018).

[40] Davis, F. J., *et al.,* "Processing Parameters" in Mitchell, G. R., ed., "Electrospinning. Principles, Practice and Possibilities, The Royal Society of Chemistry, Cambridge, UK, (2015).

[41] Beachley, V., and X. Wen, "Effect of Electrospinning Parameters on the Nano Fiber Diameter and Length," Materials Science & Engineering C, 29(3), pp. 663–668 (2009).

[42] Greiner, A., and J. H. Wendorff, "Electrospinning: A Fascinating Method for the Preparation of Ultrathin Fibers", Angew. Chem. Int. Ed., 46, pp. 5670–5703 (2007).

[43] Huang, C., *et al.,* "Electrospun Polymer Nanofibres with Small Diameters," Nanotechnology, 17, pp. 1558-1563 (2006).

[44] Zhang, S., *et al.,* applied "Influence of Solvent Selection in the Electrospraying Process of Polycaprolactone." Applied Sciences, 3(3):402 (2019).

[45] Koombhongse, P., "Effect of Solvent on Morphology of Electrospun Polystyrene Nanofiber," European Polymer Journal, 41, pp. 409-42 (2009).

[46] Luo, C. J., *et al.,* "Mapping the Influence of Solubility and Dielectric Constant on Electrospinning of Polycaprolactone Solutions," Macromolecules, 45, pp. 4669-4680 (2012).

[47] Yang, R. R., *et al.,* "Bubble-electrospinning for Fabrication of Nanofibers with Diameter of about 20 nm," International Journal of Nonlinear Sciences & Numerical Simulation, 11, pp. 163–164 (2010).

[48] Yang, Q., *et al.,* "Bubble-electrospinning for Polyacrylonitrile (PAN) nanofibers," International Journal of Nonlinear Sciences & Numerical Simulation, 11, pp. 165–169 (2010).

[49] Jacobs, V., *et al.,* "The Influence of Electrospinning Parameters on the Structural Morphology and Diameter of Electrospun Nanofibers," Journal of Applied Polymer Science, 115, pp. 3130–3136 (2010).

[50] Khalil, A., *et al.,* "Preparation and Characterization of Electrospun PLGA/silver Composite Nanofibers for Biomedical Applications," International Journal of Electrochemical Science, 8, pp. 3483-3493 (2012).

[51] Ekram, B., *et al.,* "Optimum Parameters for the Production of Nano-scale Electrospun Polycaprolactone to be Used as a Biomedical Material," Advances in Natural Sciences: Nanoscale and Nanotechnology, 8(4): 045018 (2017).

[52] Chaurey, V., *et al.,* "Interplay of Electrical Forces for Alignment of Sub-100 nm Electrospun Nanofibers on Insulator Gap Collectors," Langmuir, 26(14), pp. 19022–19026 (2010).

[53] Stoddard, R., and X. Chen, "Electrospinning of Ultra-Thin Nanofibers Achieved through Comprehensive Statistical Study," Materials Research Express, 3, 055022 (2016).

[54] Bolgen, N., *et al.,* "*In vitro* and *in vivo* Degradation of Non-Woven Materials Made of Poly(ε-caprolactone) Nanofibers Prepared by Electrospinning under Different Conditions," J. Biomater. Sci. Polymer Edn., 16(12), pp. 1537-1555 (2005).

[55] Baby, T. E, *et al.,* "A Cost Effective and Facile Approach to Prepare Beadless Polycarbonate Nanofibers with Ultrafine Fiber Morphology," Polymer Engineering and Science, 59, pp. 1799-1809 (2019).

[56] Colmenares-Roldán, G. J., *et al.,* "Influence of the Molecular Weight of Polymer, Solvents and Operational Condition in the Electrospinning of Polycaprolactone," Revista Facultad de Ingeniería, 84, 35–45 (2017).

[57] Ghobeira, R., *et al.,* "Wide-ranging Diameter Scale of Random and Highly Aligned PCL Fibers Electrospun Using Controlled Working Parameters," Polymer, 157, pp. 19–31 (2018).

[58] Han, T. T., *et al.,* "Design and Development of a Novel Nanofiber Nasal Filter (NNF) to Improve Respiratory Health," Aerosol and Air Quality Research, 18(8), pp. 2064–2076 (2018).

[59] Jian, S., *et al.,* "Nanofibers with Diameter Below one Nanometer from Electrospinning," RSC Advances, 8, pp. 4794–4802 (2018).

[60] Zhang, Q., *et al.,* "Electrospinning of Ultrafine Conducting Polymer Composite Nanofibers with Diameter Less than 70 nm as High Sensitive Gas Sensor," Material (Basel), 11(9), 1744 (2018).

[61] Zheng, J.-Y., *et al.,* "The Effect of Surfactants on the Diameter and Morphology of Electrospun Ultrafine Nanofiber," Journal of Nanomaterials, 6, 1-9 (2014).

[62] Beisbayeva, Z., "A Nanofibrous Scaffold Representative of the Change in Collagen Fibril Diameter Distribution of Bovine Anterior Cruciate Ligament upon Injury," Master's Thesis, Nazarbayev University, Kazakhstan (2019).

[63] Liu, J., *et al.,* "Single Electrospun PLLA and PCL Polymer Nanofibers: Increased Molecular Orientation with Decreased Fiber Diameter," Polymer, 118, pp. 143-149 (2017).